PHYTOCHEMICAL INVESTIGATION, BIOLOGICAL EVALUATION, AND *IN SILICO* MOLECULAR DOCKING STUDIES OF COMPOUNDS ISOLATED FROM THE ROOT EXTRACTS OF *GLORIOSA SUPERBA* LINN.

Iman Mustafa

A Thesis Submitted to the Department of Applied Chemistry

School of Applied Natural Science

Presented in Partial Fulfillment of the Requirement for the Degree of Master's in Applied Chemistry (Natural Product Chemistry)

Office of Graduate Studies

Adama Science and Technology University

July, 2023

Adama, Ethiopia

Phytochemical Investigation, Biological Evaluation, and *In Silico* Molecular Docking Studies of Compounds Isolated from the Root Extracts of *Gloriosa superba* Linn.

Iman Mustafa

Advisor: Professor Milkyas Endale

A Thesis Submitted to the Department of Applied Chemistry

School of Applied Natural Science

Presented in Partial Fulfillment of the Requirement for the Degree of Master's in Applied Chemistry (Natural Product Chemistry)

Office of Graduate Studies

Adama Science and Technology University

July, 2023

Adama, Ethiopia

DECLARATION

I hereby declare that this Master Thesis entitled "**Phytochemical Investigation, Biological Evaluation, and *In Silico* Molecular Docking Studies of Compounds Isolated from the Root Extracts of *Gloriosa superba* Linn.**" is my original work. That is, it has not been submitted for the award of any academic degree, diploma, or certificate in any other university. All sources of materials that are used for this thesis have been duly acknowledged through citation.

_____	_____	_____
Name of student	Signature	Date

RECOMMENDATION

I, the advisor of this thesis, hereby certify that I have read the revised version of the thesis entitled "**Phytochemical Investigation, Biological Evaluation, and *In Silico* Molecular Docking Studies of Compounds Isolated from the Root Extracts of *Gloriosa superba* Linn.**" prepared under my guidance by Iman Mustafa submitted in partial fulfillment of the requirements for the degree of Masters of Science in Applied Chemistry (Natural Product Chemistry). Therefore, I recommend the submission of a revised version of the thesis to the department following the applicable procedures.

Prof Milkyas Endale		19/07/2023
Major Advisor	Signature	Date

APPROVAL PAGE OF M.Sc. THESIS

I, the advisor of the thesis entitled "**Phytochemical Investigation, Biological Evaluation, and *In Silico* Molecular Docking Studies of Compounds Isolated from the Root Extracts of *Gloriosa superba* Linn**." and developed by Iman Mustafa, hereby certify that the recommendation and suggestions made by the board of examiners are appropriately incorporated into the final version of the thesis.

Prof. Milkyas Endale		19/07/2023
Major Advisor	Signature	Date

We, the undersigned, members of the Board of Examiners of the thesis by Iman Mustafa have read and evaluated the thesis entitled "**Phytochemical Investigation, Biological Evaluation, And *In Silico* Molecular Docking Studies of Compounds Isolated from the Root Extracts of *Gloriosa superba* Linn."** and examined the candidate during the open defense. This is, therefore, to certify that the thesis is accepted for partial fulfillment of the requirement of the degree of Master of Science in Applied Chemistry (Natural Product Chemistry).

Chairperson	Signature	Date
Tadesse Melaku (PhD)		19/07/2023
Internal Examiner	Signature	Date
Prof. Legesse Adane		18/07/2023
External Examiner	Signature	Date

Final approval and acceptance of the thesis are contingent upon the submission of its final copy to the Office of Postgraduate Studies (OPGS) through the Department Graduate Council (DGC) and School Graduate Committee (SGC).

Department Head	Signature	Date
School Dean	Signature	Date
Office of Postgraduate Studies, Dean	Signature	Date

ACKNOWLEDGMENT

My most profound appreciation goes to my advisor Prof. Milkyas Endale for his time, effort, patience, and understanding throughout the research duration and thesis write up. I also extend my appreciation to natural product chemistry research groups members i.e., Kebede Shenkute, Getachew Tegegn, Teshome Degife, Demis Zelelew, Bihon Abera, and Hadush G/Hiwot. I would also like to express my gratitude to Adama Science and Technology University (ASTU) for offering MSc. scholarship and financing the research work. Department of Applied Chemistry (ASTU) is also duly acknowledged for offering laboratory access and material support.

To conclude, I would like to thank God, my parents, and my friends. It would have been impossible to finish my studies without their unwavering support over the past few years.

TABLE OF CONTENTS

LIST OF TABLES

LIST OF FIGURES

LIST OF ABBREVIATIONS

ATCC	American Type Culture Collection
DMSO	Dimethylsulphoxide
DNA	Deoxyribonucleic acid
DEPT	Distortion less Enhancement by Polarization Transfer
DPPH	1,1-diphenyl-2-picryl-hydrazyl
LD_{50}	Half-maximal Lethal Dose
FDA	Food and Drug Administration
GC-MS	Gas Chromatography-Mass Spectrometry
IC_{50}	Half-maximal inhibitory concentration
MHA	Muller Hinton Agar
MIC	Minimum Inhibition Concentration
NMR	Nuclear Magnetic Resonance
TLC	Thin Layer Chromatography
UV-Vis	Ultraviolet Visible
WHO	World Health Organization

ABSTRACT

Since ancient times, medicinal plants have been used around the world to treat a wide range of ailments, diseases, and wounds. They are part of the socio-cultural legacy of different countries, evidenced by the ethnobotanical information showed in their pharmacopeias. The roots of G. superba are commonly used as an antitumor, antimicrobial, abortifacient, anthelmintic, and anti-inflammatory agent. In this study the roots of G. superba (320 g) was successively extracted with n-hexane, chloroform, and methanol to afford 530 mg (0.17%), 2.89 g (0.90%), and 17.78 g (5.56%) yields, respectively. Silica gel column chromatographic separation of the chloroform and methanol extracts afforded one caffeic acid derivative (**48**), *desmosterol* (**49**), *two phenolic derivatives* (**50**, **51**) *and two disaccharides* (**52**, **53**). *All compounds reported herein for the first time from the species. The structures of isolated compounds were characterized using NMR spectroscopic techniques (^{1}H NMR, ^{13}C NMR, and DEPT-135). The crude extracts and isolated compounds were evaluated for their in vitro antibacterial activities using the disc diffusion method against six bacterial strains. Promising inhibition zone values were observed by chloroform extract against K. pneumoniae (13±0.00 mm), S. typhimurium (13±1.00 mm), and S. aureus (12.33±0.58 mm) compared to gentamicin (15.86±4.67 mm, 28.86±2.34 mm, and 25.43±2.15 mm, respectively). Compounds **49** and **51** showed significant activities against P. aeruginosa with a mean inhibition zone of 14±1.00 mm and 14±1.73 mm, respectively, compared to gentamycin (25±2.52 mm). Compound **49** also displayed promising inhibition against S. typhimurium with a mean inhibition zone value of 15±0.00 mm. The results from DPPH activity demonstrated chloroform and methanol extracts inhibited the DPPH radical by 95.14 % and 72.98 % whereas compound **49** displayed 35.69 % inhibition. The drug-likeness analysis showed that compounds **48, 49,** and **51** to satisfy Lipinski's rule of five with zero violations. Compounds **48** and **49** showed binding affinities of -6.3 and -6.7 against E. coli and DNA gyrase B, respectively, while **49** showed -7.8 kcal/mol against PqsA, compared to amoxicillin (-6.1 kcal/mol and -7.3 kcal/mol, respectively). Therefore, the in vitro antibacterial and radical scavenging activity tests of the molecular docking analysis could suggest the potential use of the extracts of G. superba and compounds **48, 49** and **51** as promising antibacterial agents and the extracts as promising free radical scavengers.*

***Keywords*:** *Gloriosa superba*, phytochemical screening, molecular docking, antibacterial, antioxidant

1. INTRODUCTION

1.1 Background

Medicinal plants have been employed as medicine by human civilizations from the dawn of time. These are still taken by a huge portion of the world's population, particularly in developing countries, and have been proven to be beneficial in the treatment of various serious diseases, including cancer and various infections (Dar et al., 2017). They are extracted and processed for direct ingestion as herbal or traditional medicine, or research purposes. The notion of medicinal plant preparation for experimental purposes entails the correct and timely gathering of the plant, verification by an expert, suitable drying, and grinding. Following this, the bioactive component is extracted, fractionated, and isolated, if applicable. It also includes determining the quantity and quality of bioactive molecules (Abdullahi & Mainul, 2020).

The active components of these medicinal plants are usually secondary metabolites. These include classes of compounds such as alkaloids, glycosides, saponins, resins, terpenes, essential oils, etc., synthesized by biosynthetic pathways present in plant tissue having a specific physiological effect on the human body (Amritpal, 2011; Edeoga et al., 2005). These compounds are generally seen as having greater "drug-likeness and biological friendliness" than completely synthetic compounds, making them promising candidates for further research (Kumaraswamy et al., 2008). World Health Organization (WHO) also promotes herbal medicines since they have been reported to be affordable, safe, and without any severe side effects when compared to synthetic pharmaceuticals (Dar et al., 2017).

Plant species used in traditional medicine are abundant in Ethiopia. More than 80% of the population uses traditional medicine, and plant-based medicines account for more than 95% of all medicinal preparations (Abebe 1986). Ethiopia's diverse geography, variety of ecosystems and flora types, and multiethnic population encourage the cultivation and use of medicinal herbs by traditional healers to treat human and animal ailments (Gebeyahu et al., 2014; GebreEgziabher, 1991). The nation has a wide biological resource, with around 6,500 species of higher plants, roughly 12% of which are indigenous, making it one of the six plant biodiversity-rich regions (Kelbessa et al., 2000). Despite its significant contribution to society, less effort has been spent to upgrade the country's traditional health practices, and traditional medicine has gotten less attention in modern research and development (Tadeg, 2005).

Gloriosa superba L. (Family: Colchicaceae/ Liliaceae (according to the Angiosperm Phylogeny Group (**APG**) III system of classification) is an herbaceous medicinal climber that is found dispersed in several parts of Ethiopia and across Africa's tropical and subtropical regions: Senegal, Somalia, South Africa, and Zambia, as well as Southeast Asia, including India, Myanmar, Sri Lanka, and Malaysia. It is a stunning tuberous plant with bright wavy-edged yellow and red flowers that emerge especially in rainy seasons (Saraswathi et al., 2020).

G. superba has a variety of therapeutic characteristics, and each component of the plant, including tubers, leaves, seeds, and flowers, is used to cure ailments in Ayurveda and Yunani (Patil and Gavade 2012). It is rich in phytochemicals like alkaloids, glycosides, flavonoids, and saponins, which can act as antioxidants and may lower the risk of cancer and enhance heart health(Simon & Jayakumar, 2016). It is also used to treat cancer, gout, asthma, leprosy, arthritis, piles, ulcers intestinal worms, bruising, infertility, skin problems, and impotence (Nikhila, et al. 2016; Warrier, et al. 1995). Moreover, it serves as an abortifacient, anthelmintic, and anti-inflammatory agent (Nikhila et al., 2016). The tubers and seeds of this plant afforded two prominent alkaloids namely colchicine (**1**) and colchicoside (**9**) of which the former was known for its anti-cancer activity (Bharathi et al., 2006). This study was intended to investigate the chemical constituents of the roots of the plant, examine their antibacterial and antioxidant activity along with *in silico* molecular docking and drug likeness properties of the compounds.

1.2 Statement of the Problem

Bacterial diseases are responsible for a large proportion of health issues in developing countries. Many synthetic antibiotics are routinely used to treat bacterial diseases. Because of the indiscriminate use of synthetic antibiotics, bacteria have developed resistance to many antibiotics, causing enormous clinical problems in the treatment of infectious diseases. The ongoing emergence of multidrug-resistant bacteria, as well as the infectious diseases caused by them, is a major global concern. As a result, there is a continuous and urgent need to develop new antimicrobial compounds with diverse chemical structures and novel mechanisms of action for the treatment of infectious diseases caused by multidrug-resistant microorganisms, as well as stress-related diseases and disorders. Medicinal plants are important sources of plant-derived phytochemicals that are active against various diseases and for eco-friendly applications. However, there are few studies on Ethiopian medicinal plants' antimicrobial capabilities, their efficiency against disease-causing pathogens, and their potential for use in drug development.

G. superba is a good source of phytochemicals like alkaloids, glycosides, flavonoids, and saponins (Simon and Jayakumar 2016). In Ethiopia, there isn't any published research paper on the antibacterial, antioxidant activity, and phytochemical analysis of this plant. Nevertheless, the local people still use it to treat various ailments (Itefa & Tolessa, 2016). Thus, this project aims to identify the chemical constituents found in the roots of the plant and examines the effectiveness of crude extracts as well as compounds against various bacterial strains and their antioxidant activities along with computational study to know the molecular interaction of active compounds against selected protein targets.

1.3 Objectives of the Study

1.3.1 General Objective

The overall objective of this study is to extract, isolate and characterize the chemical constituents present in the root extracts of *G. superba,* evaluate their biological activities and *in silico* molecular docking interactions of isolated compounds with selected protein domains.

1.3.2 Specific Objectives

The specific objectives of the study are as follows:

- To extract the roots of *G. superba* using *n*-hexane, chloroform and methanol followed by isolation of compounds from the crude extracts by using column chromatography technique.
- To elucidate the structure of isolated compounds using spectroscopic method (^{1}H NMR, ^{13}C NMR, and DEPT-135) and comparison with literature data/reports.
- To test the antibacterial activities of the extracts and isolated compounds using disk diffusion method against selected bacterial strains (*Escherichia coli, Staphylococcus aureus, Enterococcus faecalis, Pseudomonas aeruginosa, Klebsiella pneumonia, and Salmonella typhimurium)*
- To examine antioxidant activities of the extracts and isolated compounds using DPPH radical scavenging method
- To conduct *in silico* molecular docking study of active compounds using Auto Dock vina 4.2 against selected protein targets (DNA gyrase B, pyruvate kinase, PqsA, and human peroxiredoxin 5) protein targets
- To predict ADMET of isolated compounds using SwissADME and Pro Tox II online servers

1.4 Significance of the Study

This study is expected to provide:

- Documentary information about chemical constituents, and biological activity of *G. superba* to provide scientific support to traditional uses of the selected medicinal plant;
- Information for a better understanding of the molecular mechanisms of interactions between the compounds with promising activity on selected protein targets of microorganisms
- Baseline information for future related scientific studies on medicinal plants.

2. LITERATURE REVIEW

2.1 Family Colchicaceae

Colchicaceae (Liliales) are rhizomatous or cormous perennials that have been traditionally divided into two subfamilies, though this division, as well as the phylogenetic ties between family members and sister relationships, is still being debated. This family comprises approximately 250 species and 15-21 genera found in temperate and tropical Africa, Europe, Asia, Australia, and North America (Thi et al., 2013); the most abundant being in South Africa's temperate zones (Sebsebe & Inger, 2010). According to Sebsebe and Inger (2010) 5 genera and 7 indigenous species are known to exist in Ethiopia and Eritrea. The biosynthesis of colchicine is demonstrated originating within the common ancestors of this family, as stated in the study of the re-circumscribed and extended Colchicaceae family. This made the tropolone alkaloid colchicine to be considered as a synapomorphy trait for the family(Annika & Sonny, 2010).

2.2 Botanical Description of Genus *Gloriosa*

Gloriosa is a genus of 15 species found in South Africa, tropical Africa, Arabia, and tropical Asia. *G. superba* and *G. baudii* are two of the species that can be found in Ethiopia (Sebsebe & Inger, 2010). This genus contains perennial herbs that climb or scramble over other plants with the aid of tendrils at the ends of their leaves which are distichously arranged are cauline, sessile or shortly stalked, and often sheathing, and can reach 3 meters in height. It has tunicate underground corms with fibrous roots; annual, leafy, and glabrous stems; pendulous, nodding, or sometimes resupinate and brightly colored flowers that are straight or recurved apically (Maroyi & L.J.G.van der, 2012).

In general, this genus can be distinguished from the rest of the family by its scandent habit, a conspicuous and attractive mix of yellow, orange, and red flowers and leaves that end in tendrils (Sebsebe & Inger, 2010). 11 species of *Gloriosa* (**Table 1**) were approved into the World Checklist of Selected Plant Families in October 2018, excluding hybrids, variations, and cultivars. Many more names have been rejected as synonyms or are still unresolved due to a lack of information (*Kew Science Royal Botanical Garden, 2018*).

Table 1: Different species of genus *Gloriosa* and their distribution.

Species	Distribution
Gloriosa baudii (A.Terracc.) Chiov.	Ethiopia, Somalia, Kenya
Gloriosa carsonii Baker	Central, Eastern, and Southern Africa
Gloriosa flavovirens (Dammer) J.C.Manning&Vinn.	Angola
Gloriosa lindenii (Baker) J.C.Manning&Vinn.	Central and South EasternAfrica
Gloriosa littonioides (Welw. ex Baker) J.C.Manning&Vinn.	Central and SC Africa
Gloriosa modesta (Hook.) J.C.Manning&Vinn.	Southern Africa
Gloriosa revoilii (Franch.) J.C.Manning&Vinn.	North-Eastern Africa, Yemen
Gloriosa rigidifolia (Bredell) J.C.Manning&Vinn.	Limpopo
*Gloriosa sessiliflora*Nordal& Bingham	Angola, Zambia, Caprivi
Gloriosa simplex L.	sub-Saharan Africa, Madagascar
Gloriosa superba L.	sub-Saharan Africa, Madagascar, Seychelles, Indian Subcontinent, SE Asia, Ethiopia

2.3 Botanical Description of *G. superba*

Gloriosa superba (Vernacular name: Ililiabrasha/Hoomaa (Oromiffa) and Glory lily/ Flame lily (English)) belongs to the Colchicaceae family of flowering plants (**Figure 1**). It means "full of glory," and the specific epithet "superba" refers to the showy red and yellow flowers. Linnaeus described it in 1753 based on a plant collected by Hermann from Malabari, India (Sebsebe& Inger, 2010). *G. superba* is a stunning semi-woody herbaceous lasting creeper that grows to a height of 6 meters. During the rainy season, it grows from a tuberous underground stem. The plant can be found in *Acacia-Commiphora* and *Combretum-Terminalia* woodlands, open forest areas, thickets on roadside ditches and ditches between 500 and 2000 m, river edges, and sandy-loam soil. It is common in tropical Africa, southern Africa, Madagascar and tropical Asia, as well as Ethiopia and Eritrea. Ethiopia's main flowering season this plant species is from May to September (Maroyi, 2012; Sebsebe and Inger, 2010).

Figure 1: *Gloriosasuperba* Linn. (Phototaken by Iman Mustafa on September, 2021 from Doba, Western Hararge)

2.4 Ethnobotanical Uses of *G. superba*

G. superba is a key ingredient in Ayurvedic and Yunani medicines to treat leprosy, piles, fistula, gout, gynecological disorders, burn wounds, goiter, lymphadenitis, scrofula, hair loss, insect bite, oral diseases, vitiligo, intestinal disorders, cough, inflammatory disease, gout, ulcers, hemorrhage, cardiomyopathy, and snakebite. It is also reported to exhibit anthelmintic, laxative, alexiteric and abortifacient potential. This plant also has Rasayana properties, which means it can be used as a tonic and rejuvenator (Bhargav & Rabinarayan, 2012; Sachin et al., 2019). The tuber powder was used successfully to treat paralysis, rheumatism, snakebite, insect bites, lice, intermittent fevers, wounds, anti-fertility, gonorrhea, leprosy, piles, debility, dyspepsia, hemorrhoids, helminthiasis, and inflammations (Jana & Shekhawat, 2011; Pulliah, 2002). It can also be used to treat cholera, colic, kidney problems, typhus, itching, sprains, impotence, smallpox, sexually transmitted diseases, and a variety of endo-parasitic diseases. However, when administered in a high dose the tuber is very toxic (Tulika & Pallavi, 2020).This plant is being used traditionally in Ethiopia to treat breast cancer. Its root part is chewed and applied externally to the affected breast (Ayele,

2018). Its crushed leaf filtrate is taken orally to treat Epilepsy (Belayneh & Bussa, 2014). Moreover, the plant is used to treat snakebite, impotence, stomachache, gout and tumor (Hassan & Roy, 2005; Solomon et al., 2020).

2.5 Chemical Constituents of *G. superba*

Tubers are immensely toxic due to the presence of a highly active alkaloids such as colchicine (**1**) and gloriosine (**2**) (**Figure 2**) (C. Sachin, et al. 2019). Svatava, et al. (1984)also reported isolation of alkaloids such as cornigerine (**3**), (S)-(+)-floramultine (bechuanine) (**4**), 1,12-dihydroxy-2,10,11-trimethoxyhomoaporphine (**5**), colchicamide (**6**), 2-demethylcolchifoline (**7**), 3-demethylcolchifoline (**8**), colchicoside (**9**), and isoperlolyrine (**10**) (**Figure 2**) from the corms and seeds of Indian *G. superba* L. (Svatava et al., 1984).

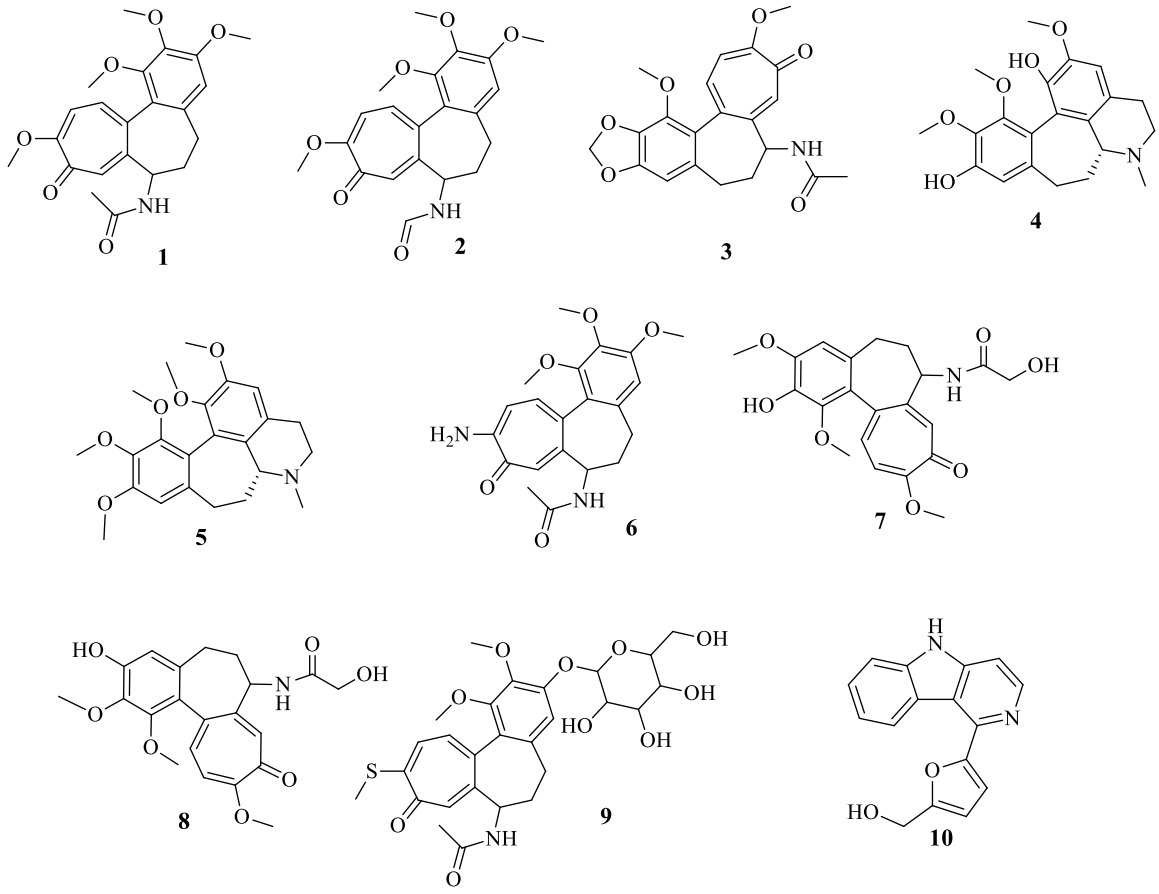

Figure 2: The chemical structures of compounds **(1-10)** isolated from corms and seeds of *G. superba*

According to Shanmugam et. al., (2009), phytochemical studies of dried roots of *G. superba* displayed the presence of long-chain fatty acids, flavonoids, tannins, glycosides, glucoside, flucoside, and alkaloids such as **1**,**2**,**9**, 3-O-demethylcolchicine-3-O-α-D-glucopyranoside (**11**), 1,2-didemethyl colchicine (**12**), β and γ-Lumicolichicines (**13** and **14**), β-sitosterol (**15**), 2,3-didemethyl colchicine (**16**), luteolin (**17**), N-formyl deacetyl colchicines (**18**),2-hydroxy-6-methoxy benzoic acid (**19**) and salicylic acid (**20**)(**Figure 3**) (Shanmugam et al., 2009).

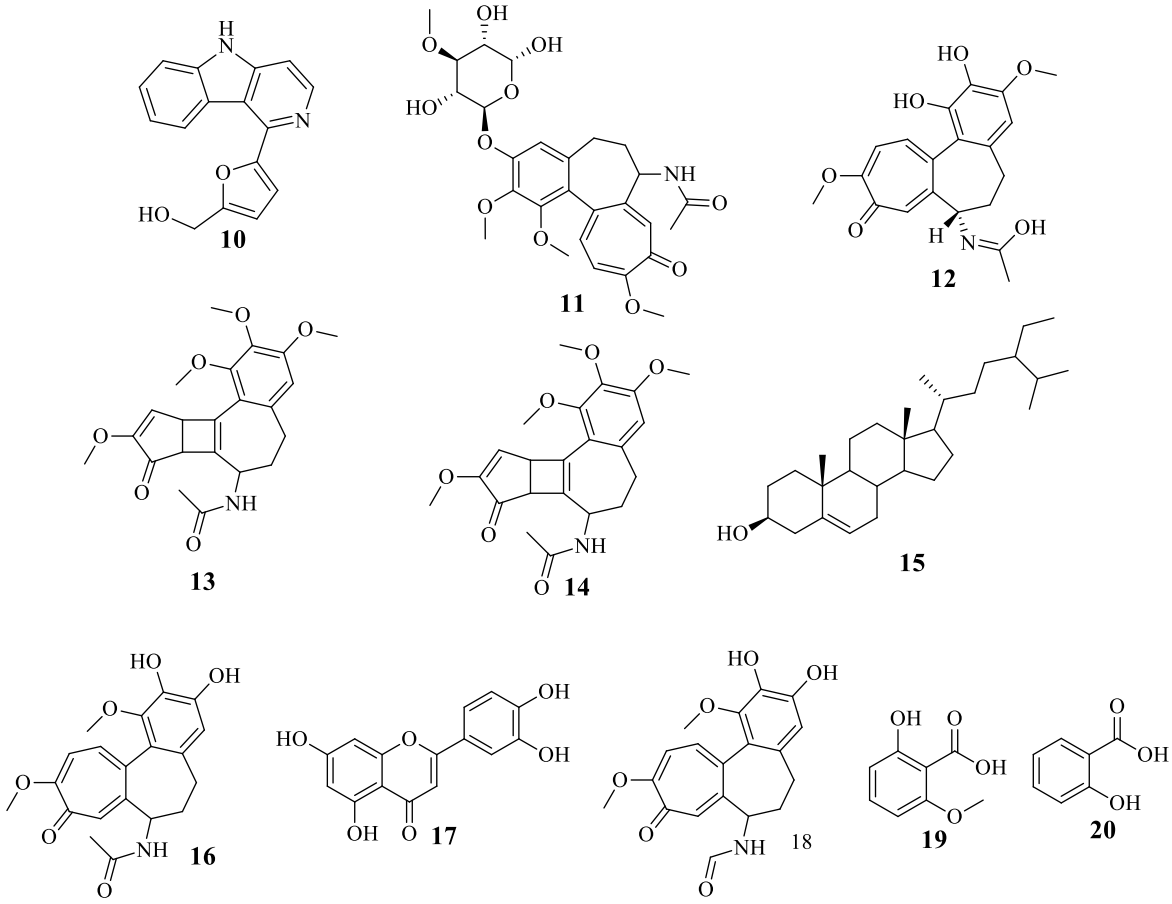

Figure 3: The chemical structures of compounds **(11-20)** isolated from roots of *G. superba*

Isolation of four glycosylated colchicinoids N-Deacetyl-N-formyl-3-de-O-methylcolchicine-3-O-β-D-glucopyranoside (glorioside) (**21**), 3-De-O-methylcolchicine-3-O-β-D-glucopyranosyl-(1→6)-3-O-β-D-glucopyranoside (colchicodiside A) (**22**), N-Deacetyl-N-formyl-3-de-O-methylcolchicine-3-O-β-D-glucopyranosyl-(1→6)-3-O-β-D-glucopyranoside (gloriodiside) (**23**), and 3-De-O-methylcolchicine-3-O-β-D-glucopyranosyl-(1→3)-3-O-β-D-glucopyranoside (colchicodiside B) (**24**) were isolated for the first time from a plant source together with **9** and 3-de-O-methylcolchicine-3-O-β-D-glucopyranosyl-(1→4)-3-O-β-D-glucopyranoside (colchicodiside C) (**25**) from the seeds of *G. superba* (**Figure 4**) (Yancho et al., 2017).

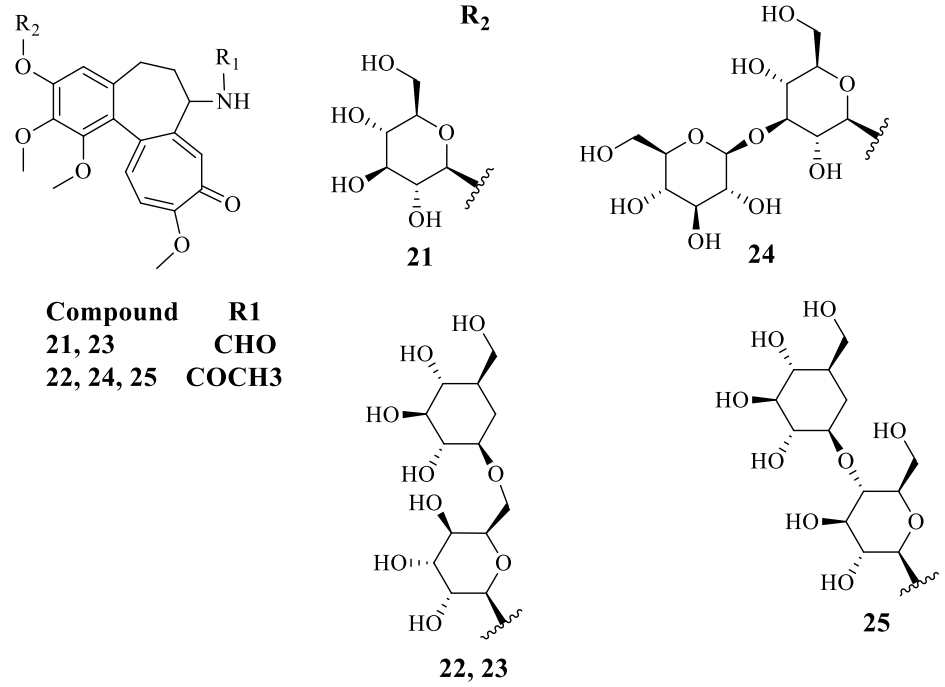

Figure 4: The chemical structures of glycosylated colchicinoids **(21-25)** isolated from seeds of *G. superba*

Flavonoids such as rutin (**26**), coumaric acid (**27**), hesperidin (**28**) and vanillic acid (**29**) were isolated from the methanolic extract of *G. superba* tuber (Sanjay & Rajendra, 2014).Nikahila et. al., (2016) also identified seventeen various classes of compounds (**30-46**) from the defatted methanolic extract of the tuber using GC-MS (**Figure 5**). The compounds are 2-methoxy-4-vinylphenol (**30**), 3-hydroxy-4-methoxymandelic acid (**31**), benzene,1,2,3-trimethoxy,5,2-propenyl (**32**), benzoic acid, 2-hydroxy ethyl ester (**33**), phenol- 2,6-dimethoxy (**34**), 1-adamantane carboxylic acid (**35**), 1-(2-methyl-4-propoxy-phenyl ethenone (**36**), 1-butanone-1-(2,4,5 trihydroxy phenyl) (**37**), 2h-1-benzopyran-3,5,6,8 tetrahydro (**38**), benzene propanoic acid (**39**), pentadecanoic acid (**40**), 1-fluoroforskolin (**41**), bicyclo[3.2.0]hept-2-ene (**42**), 3,5-dimethoxy-4-hydroxycinnamaldehyde (**43**), 7-hydroxycadalene (**44**), 9,11-octadecadienoic acid (**45**), β-amyrin trimethylsilyl ether (**46**)(**Figure 5**).The authors also reported that the compounds possess antimicrobial, antipyretic, anti-inflammatory, antitumor and hepatoprotective properties (Nikhila et al., 2016).

Recently, a new colchinoid compound, identified as *N*-deacetyl-*N*-formyl cornigerine (**47**), named glorigerine was isolated from the roots of *G. superba*. It was found to have moderate cytotoxicity when tested against four human cancer cell lines (Bharat, et al. 2022).

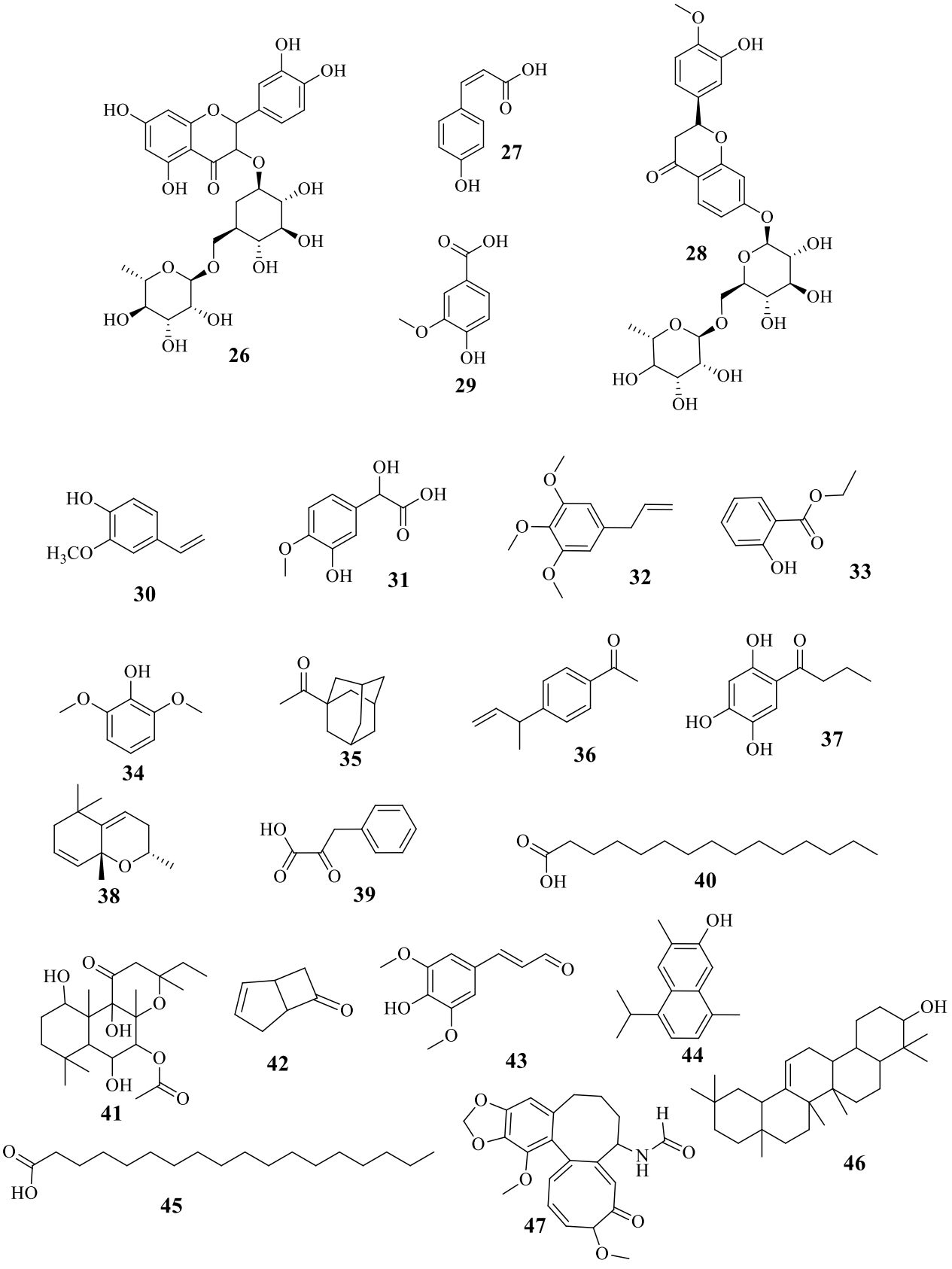

Figure 5: The chemical structures of compounds **(26-47)** isolated from tuber of *G. superba*

2.6 Pharmacological Study of *G. superba*

G. superba has traditionally been used for the treatment of various diseases (Section 2.4). Medicinal uses of *G. superba* are closely linked to the main secondary metabolites such as tropolone-type alkaloids present in the seeds and tubers(Sanjay & Rajendra, 2014). In this section, reported pharmacological activities of the plant are briefly discussed.

2.6.1 Antimicrobial Activity

Khan et al., (2008) reported that n-butanol fraction showed excellent antifungal potential against *C. albicans* and *C. glaberata* (up to 90%) and against *Trichophyton longifusus* (78%) followed by chloroform fraction against *Microsporumcanis* (80%). The chloroform fraction demonstrated highest antibacterial activity against *S. aureus* (69.4%)(Khan et al., 2008). In another study, it is reported that phytochemical extracts of DMSO, EtOAc, and EtOH from shoot, flower, and tuber of *G. superba* to be effective against *C. albicans, C. krusei, A. niger, R. oryzae*, and *Mucor* sp. EtOH solvent extracts of the tuber of *G. superba* showed the highest inhibitory activity against selected fungi than DMSO and EtOAc (Jothi, et al. 2019).

The *in vitro* antibacterial activity study done by Senthilkumar (2013) revealed that the methanol extract of *G. superba* had significant activity against the tested microorganisms, mainly *B. cereus, E. coli, S. fecalis, K. pneumonia, S. aureus, and P. aeruginosa* (zone of inhibition >30 mm) but inactive in lower concentration (50 µl) on *S. typhi*. The chloroform extracts possessed moderate activity against *B. cereus, S. fecalis, E. coli, K. pneumonia S. aureus* and *P. vulgaris* (zone of inhibition >20 mm), but was found to be inactive against *P. aeruginosa, P. vulgaris and S. typhi*. The hexane extract of *G. superba* exhibited only weak activity against *S. typhi, P. vulgaris, B. subtilis, S. aureus, S. cremoris and P. aeruginosa.* These activities were compared with the standard antibiotic drug ampicillin which showed moderate inhibition activity against *B. cereus, S. fecalis, S. aureus, E. coli, and K. pneumoniae* (Senthilkumar 2013).

According to Uchimahali et al. (2019) organic solvents (DMSO, EtOAc, and ETOH) extracts of tuber of *G. superba* displayed significant antibacterial activities than shoot and flower extracts. The maximum zone of inhibition (19.00±0.45 mm) was exhibited by EtOH (125 µL/ml in concentration) tuber extract of *G. superba* against *S. aureus* (Uchimahali et al. 2019).

2.6.2 Enzyme Inhibition Activity

Investigation on a crude extract of *G. superba* rhizomes for enzyme inhibition activities, such as lipo-oxygenase, acetylcholinesterase, butyrylcholinesterase & uricase, resulted in an extraordinary inhibition on lipo-oxygenase. The maximum enzyme inhibition potency was obtained by 90% chloroform extract among all the tested extracts. 60-70%, 49-69%, and 10-33%inhibition was obtained for lipo-oxygenase, acetylcholinesterase, and butyryl cholinesterase respectively. The extract showed no inhibitory activity for uricase (Khan, et al. 2007).

2.6.3 Analgesic and Anti-Inflammatory Activities

The analgesic and anti-inflammatory activities of a hydroalcoholic extract obtained from dried aerial parts of *G. superba* was investigated using Eddy's hot plate method and acetic acid induced writhing method for analgesic potential; cotton wool granuloma and carrageenan induced paw edema model for anti-inflammatory activity. According to the study, mice treated with 100, 200, and 400 mg/kg body weight had a substantial ($P<0.01$) increase in reaction time. For all three doses, the highest percentage protection was found at 90 minutes. At doses of 100, 200, and 400mg/kg body weight, the percent inhibition of writhes was 64.09 %, 78.56 %, and 81.45 %, respectively. In the carrageenan induced paw edema model, the doses of 200 and 400 mg/kg produced significant outcomes ($P<0.05$) when compared to the control. After 7 days of therapy with doses of 100, 200, and 400 mg/kg body weight, the rats showed 9.59 %, 28.72 %, and 45.8% suppression of granuloma mass formation (John, et al. 2009).

Maroyi and Maesen, (2012) reported alcoholic, hydroalcoholic and aqueous extracts of *G. superba* tubers have shown to have significant anti-inflammatory activity in male albino rats. According to the study, aqueous extract of 250 mg/kg of *G. superba* tubers showed the best anti-inflammatory activity. Oral administration of colchicine at 2, 4 and 6 mg/kg body weight resulted in 48.9, 68.7 and 79.1% inhibition respectively, while 30.9% inhibition was obtained in the phenylbutazone 100mg/kg treated group once daily for a period of 4 days. These results clearly indicate that colchicine is more effective as an anti-inflammatory agent (Maroyi and Maesen 2012).

2.6.4 Neuroprotective Activity

Hydroalcoholic extract obtained from tubers of *G. superba* showed a decrease in the transfer latencies, and strengthened its memory improvement action in drug treated rats. Consequently, it showed improvement in muscle strength. The locomotor activity assessed by acto-photometer and open field test was decreased in lead nitrate group compared with hydroalcoholic extract treated group. Biochemical analysis of brain revealed that the chronic administration of lead nitrate significantly increased lipid peroxidation and decreased levels of catalase (CAT), reduced glutathione (GSH) and glutathione reductase (GR), an index of oxidative stress process. Administration of hydroalcoholic extract of *G. superba* attenuated the lipid peroxidation and reversed the decreased brain CAT and GSH levels. Lead exposed rats showed increased levels of various serum parameters like glucose, ALT, ALP, TG and TC28(Rani, et al. 2016).

2.6.5 Anti-Cancer Activities

Simon et al. (2016) reported the anticancer activity of phytochemical extract obtained from tubes of *G. superba* against Hep-G2 cancer cell line (Human liver cancer cells) employing MTT assay. The study revealed that concentration of 100µg of plant extract has maximum inhibition value of 54.3% against Hep-G2 cancer cell line (Simon et al. 2016). Four fractions of *G. superba* L., i.e., *n*-hexane, dichloromethane, and methanol fractions were investigated for colchicine-like activity using a mosquito cytogenetic assay. The results revealed that the latter fractions yielded promisingly high colchicine-like activity, whereas the *n*-hexane fraction yielded very low activity compared with 1% colchicine in a 0.85% sodium chloride solution (Amritpal 2011). Uniformly spherical and almost isodiametric Monodispersed PtNPs and PdNPs were synthesized using *G. superba* tuber extract which showed potent anticancer activity against MCF-7 (human breast adenocarcinoma) cells. The mechanism of cell death was confirmed to be an induction of apoptosis characterized by phosphatidyl serine externalization, membrane disintegration, and blebbing with chromosome condensation (Shalaka, et al. 2018).

3. MATERIALS AND METHODS

3.1 Plant Material Collection and Identification

The plant material was collected from Doba district, Western Hararge Zone. The area is located about 378 km to the east of Addis Ababa. The identification of the plant material was done with the help of Botanist Melaku Wendaferash at the Department of Biology, National Herbarium of Ethiopia, Addis Ababa University (voucher code: IM001).

3.2 Materials and Chemicals

Column chromatography was carried out using silica gel (60-120 mesh) ASTM. Thin Layer Chromatography (TLC) was performed using pre-coated aluminum-backed supported silica gel $60F_{254}$ (0.2 mm thickness). ^{1}H and ^{13}C NMR spectra were recorded on a Bruker Avance 400 MHz spectrometer with TMS as the internal standard and $CDCl_3$ and DMSO-$d_6$as solvents.

Chemicals that were used for extraction, isolation, phytochemical analysis, and other activities were silica gel (Loba Chemie PVT. LTD., 60-120 mesh), ethanol (Favor trading PLC, 99.9%), methanol (CDH (P) Ltd., 99.8%), chloroform (CDH (P) Ltd., 99.8%), *n*-hexane (Loba Chemie PVT.LTD., 99%), ethyl acetate (Loba Chemie PVT. LTD., 99.5%), dichloromethane (Loba Chemie PVT. LTD., 99.5%), ammonium solution (Avi chem, 25%), ferric chloride (Sigma Aldrich, 97%), sulfuric acid (Loba Chemie PVT. LTD., 98%), hydrochloric acid (Loba Chemie PVT. LTD., 35.4%), DPPH, DMSO (Srlchem, 99.5%), Potassium Iodide (Samir Tech-Chem PVT. LTD., 99.8%), Iodine (Alpha Chemika, 98.5%), and distilled water.

3.3 Preparation of Plant Material and Extraction

3.3.1 Preparation of Plant Material

The collected rhizomes of *G. superba* were cut into smaller pieces and dried under shade. Then it was pulverized into a fine powder using a mechanical grinder. The powder was stored in airtight containers at room temperature till further experimentation.

3.3.2 Extraction

The root powder of *G. superba* (320 g) was soaked into *n*-hexane (2L) for 72 hrs. and shaken with mechanical shaker at room temperature. The solution was filtrated and concentrated using a rotary evaporator at around 40^{o}C to afford *n*-hexane crude extract. The marc left was soaked in chloroform (2L) for72 hrs. The mixture was filtered, and dried to afford chloroform crude extract.

Finally, the marc left was further extracted in methanol (2L) for 72 hrs. followed by filtration and dried to afford methanol crude extract. The extracts' TLC profiles were checked to identify appropriate eluent for column chromatographic separation.

3.4 Phytochemical Screening

Phytochemical examinations were carried out for *G. superba* extracts as per the standard methods.

Test for Alkaloids (Wagner's test): The methanol extract (30 mg) was separately stirred with 1% HCl (0.5 mL) in a water bath for 5 min and filtered into a test tube. 1 mL of Wagner's reagent (Iodine in Potassium Iodide) was added; the formation of a brown/reddish precipitate indicates the presence of alkaloids (Praiwala *et al*., 2019).

Test for flavonoids: The methanol extract (30 mg) was dissolved in 10 mL of ethyl acetate and heated for 3 min using a steam bath. The mixture was filtered, and to the filtrate 1mL of dilute ammonia solution was added. The formation of intense yellow color ratifies the presence of flavonoids (Mir *et al.*, 2016a).

Test for Phenols: The methanol extract (30 mg) was dissolved in 5mL of distilled water. To this, a few drops of neutral 5% ferric chloride solution was added. A dark green color indicated the presence of phenolic compounds (Bargah & Rohit, 2015).

Test for Tannins: The methanol extract (30 mg) was dissolved in 5mL of distilled water, filtered and ferric chloride reagent was added to the filtrate. A blue-black, green, or blue-green precipitate was taken as evidence of the presence of tannins (Mir *et al*., 2016b).

Test for Terpenoids (Salkowski's Test): The methanol extract (30 mg) was dissolved in 2 mL of chloroform and concentrated H_2SO_4 (3 mL) was carefully added to form a layer. An appearance of reddish brown color on the inner face indicated the presence of terpenoids (Santhi & Sengottuvel, 2016).

Test for saponins: The methanol extract (30 mg) was dissolved in 5 mL of distilled water and shaken while heating to boil. Frothing showed the presence of saponins (Kamal *et al*., 2012).

Test for Steroids: The methanol extract (30 mg) was dissolved in 10 mL of chloroform and an equal volume of concentrated H_2SO_4 was added by the sides of the test tube. A reddish-brown color at the interphase indicates the presence of a steroidal ring (Nwodo & Nkwocha, 2015).

3.5 Isolation of Compounds

The crude extracts of chloroform and methanol were combined as they showed similar TLC profiles. The combined crude extract (15 g) was adsorbed onto15 g of silica gel (mesh size 60-120), and subjected to silica gel column chromatography (165 g of silica gel) using *n*-hexane for initial packing. Elution was carried out with increasing gradient of ethyl acetate in *n*-hexane followed by increasing gradient of methanol in dichloromethane. A total of 171 fractions (50 mL each) were collected. Fractions that showed identical R_f values and the same characteristic color on TLC were combined.

Fraction 10 (eluted with 20% EtOAc in *n*-hexane) was washed with *n*-hexane and afforded compound **48** (14.4 mg) as white powder. Fraction 13 (eluted with 30% EtOAc in *n*-hexane) afforded compound **49** (14.2 mg) as pale-yellow powder. Fraction 16 and 17 (eluted with 30% EtOAc in *n*-hexane) combined to afforded compound **50** (17.4 mg) as a pale-yellow needle-like compound. Fractions 35-40 (eluted with 40% EtOAc in *n*-hexane) were combined and washed with *n*-hexane to afford compound **51** (12.8 mg) as pale-yellow needles. Fractions 165 and 168 (eluted with 100% methanol) afforded compound **52** (100.8 mg) as white powder and compound **53** (169.3 mg) as reddish-brown powder after washing the crude extractswith DCM (**Table 2**).

Table 2: Summary of fractionation of chloroform-methanol crudeextracts

Solvent System	Ratio	Fractions	Solvent System	Ratio	Fractions
n-hexane	100:0	$F_1 – F_2$	DCM	100	$F_{132} – F_{133}$
n-hexane: EtOAc	98:2	F_3	DCM: MeOH	98:2	$F_{134} – F_{135}$
	95:5	F_4		95:5	F_{136}
	90:10	F_5		90:10	$F_{137} – F_{152}$
	85:15	F_6		85:15	F_{153}
	80:20	$F_7 – F_{10}$		80:20	F_{154}
	75:25	F_{11}		75:25	F_{155}
	70:30	$F_{12} – F_{17}$		70:30	$F_{156} – F_{158}$
	65:35	$F_{18} – F_{20}$		60:40	$F_{159} – F_{160}$
	60:40	$F_{21} – F_{40}$		50:50	$F_{161} – F_{163}$
	55:45	$F_{41} – F_{43}$		40:60	F_{164}
	50:50	$F_{44} – F_{46}$	MeOH	0:100	$F_{165} – F_{171}$
	40:60	$F_{47} – F_{63}$			
	30:70	$F_{64} – F_{82}$			
	80:20	$F_{83} – F_{88}$			
	90:10	$F_{89} – F_{95}$			
EtOAc	0:100	$F_{96} – F_{131}$			

3.6 Structural Elucidation

The NMR spectroscopic techniques were employed to elucidate the structure of isolated compounds. The ^{1}H NMR, ^{13}C NMR, and DEPT-135 were obtained using Bruker Avance 400 MHz spectrometer at the Department of Chemistry, Addis Ababa University. Solvents DMSO (*d-6*) and $CDCl_3$ were utilized for the analysis.

3.7 Biological Activity

3.7.1 Antibacterial Activity

In vitro antibacterial activities of the crude extracts and isolated compounds of *G. superba* were studied against six pathogenic bacterial strains retrieved from Adama Public Health Research and Referral Laboratory Center. The strains used in the experiment were*E. faecalis* (ATCC 29212), *S. aureus* (ATCC 25923), *E. coli* (ATCC 25922), *K. pneumoniae* (ATCC 700603), *P. aeruginosa* (ATCC 27853), and *S. typhimurium* (ATCC 13311)).

In the experiment, Mueller-Hinton agar plates were inoculated with the standardized inoculum of the test micro-organisms (corresponding to 0.5 McFarland turbidity standard). Six sterile filter paper disks (Whatman No. 1 of approximately 6 mm in diameter) were impregnated with 20 µL of desired concentrations of either the crude, isolated compounds or controls (gentamicin as positive control and DMSO as negative control), and placed on the inoculated agar surface. These plates were incubated under suitable conditions, at 37°C for 24 hrs (CLSI 2018, EUCAST 2019). The diameter of the growth inhibition zones around each disc was then measured in millimeters using a sliding caliper. The experiment was done in triplicate, and the results were expressed as mean ± standard deviation.

3.7.2 Antioxidant Activity

Antioxidant activities of the extracts and isolated compounds was measured based on their free radical scavenging activity, which was determined by the 1,1-diphenyl-2-picryl-hydrazyl (DPPH) method. DPPH solution (0.04%) was prepared in methanol by dissolving 0.004 g DPPH in 100 mL methanol. The solution was kept in darkness for 30 min to complete the reaction. The crude extracts and isolated compounds were serially diluted as 1000, 500, 250, 125 µg/mL (crude extracts) and 100, 50, 25, 12.5 µg/mL (isolated compounds). To each 1 mL of serially diluted solutions4 mL of 0.04% DPPH was added to give 200, 100, 50, 25 µg/mL (crude extracts) and 20,

10, 5, 2.5 µg/mL (isolated compounds). The resulting solutions were placed in the dark for 30 minutes and then subjected to a UV-Vis spectrophotometer to record absorbance at 517 nm. Ascorbic acid with a similar concentration of test samples was used as the positive control. The DPPH radical scavenging activity of each of the tested compounds was reported by percentage inhibition using the following formula (Brand-Williams, et al. 1995):

$$\% \text{ of radical scavenging activity} = \frac{Ab_{standard} - Ab_{analyte}}{Ab_{standard}} \times 100$$

3.8 *In silico* Molecular Docking Studies of Isolated Compounds

A molecular docking study was carried out to evaluate the manner of binding of the most effective drugs against target proteins by docking isolated compounds (**47-50**) into the active site of proteins using AutoDock Vina and a standard protocol (Seeliger and de Groot, 2010, Trott and Olson 2010). The chemical structures of compounds **47-50** were drawn with the ChemOffice tool (Chem Draw 16.0) and assigned with the proper 2D orientation, and the energy of each molecule was minimized with ChemBio3D. The energy-minimized ligand molecules were then fed into AutoDock Vina to perform the docking simulation. The protein data bank was used to download the crystal structures of the receptor molecules DNA gyrase B of *E. coli* (PDB ID: 6F86), PqsA of *P. aeruginosa* (PDB ID:5OE3), pyruvate kinase of *S. aureus* (PDB ID:3T07), and human peroxiredoxin 5 (PDB ID: 1HD2).

Using the reported standard protocol, the protein was prepared by removing the co-crystallized ligand, selected water molecules and cofactors. The target protein file was prepared by leaving the associated residue with protein using Auto Preparation of target protein file Auto Dock 4.2. (MGL tools1.5.7). The grid box for docking simulations was set using the graphical user interface program. The grid was designed to surround the region of interest in the macromolecule. To find the best-docked conformation between ligand and protein, the docking algorithm provided with AutoDock Vina was used. For each ligand, a maximum of nine conformers were considered during the docking process. Conformations with the most favorable (least) free binding energy were selected for analyzing the interactions between the target receptor and ligands by Discovery studio visualizer and PyMOL. The ligands were represented by different colors, while the H-bonds and interacting residues were represented by stick models (Narramore et al. 2019).

3.9 *In silico* Drug-Likeness and Toxicity Predictions

The isolated compounds were evaluated for their pharmacokinetic profiles by *insilico* methods for predicting their molecular properties using Lipinski's Rule of Five (Lipinski 2016) and the Veber rule (Veber et al. 2002). The physicochemical and pharmacokinetics properties of the compounds were estimated using ADME descriptors by SwissADME (http://www.swissadme.ch/), online server. To estimate *in silico* and pharmacokinetic parameters and other molecular properties, the isolated compound structures were submitted to SwissADME tools and converted to their canonical simplified molecular-input line-entry system "SMILEs". The organ toxicity profiles and toxicological endpoints of the isolated compounds and toxicity classes were predicted using the Pro Tox II web server explore (https://toxnew.charite.de/).

4. RESULTS AND DISCUSSION

4.1 Extraction Yield

The plant materials (roots) of *G. superba* were successively extracted with *n*-hexane, chloroform, and methanol to afford 530 mg (0.17%), 2.89 g (0.90%), and 17.78 g (5.56%) yields, respectively. The latter extract was found to be light brown, the middle one to be brick red and the first one was yellow in color. The extraction yield obtained using methanol solvent was higher compared to *n*-hexane and chloroform extracts suggesting the roots of the plant contain polar secondary metabolites (World Health Organization||WHO Expert Committee on Specifications for Pharmaceutical Preparations 2018).

4.2 Phytochemical Screening

Phytochemical screening tests were performed to determine the class of chemicals present in the crude extracts. These tests revealed the presence of alkaloids, flavonoids, tannins, steroids, saponins, terpenoids, and phenol where alkaloids were found to be absent in *n*-hexane extract (**Table 3**) in agreement with Rehana and Nagarajan (2012) who reported the presence of alkaloids, flavonoids, tannins, steroids, saponins, terpenoids, and phenols in chloroform and methanol extracts of tubers of *G. superba* (Rehana and Nagarajan 2012).

The study undertaken by Jothi, et al. (2019) confirmed the presence of alkaloids, flavonoids, terpenoids, tannins, saponins, aromatic acids, phenolic compounds, xanthoproteins, triterpenoids, amino acids, carbohydrate, reducing sugar, and proteins in tuber extracts, while reducing sugars, xanthoproteins, amino acids, carbohydrate, reducing sugar, and proteins were absent. *G. superba* shoot, flower, and tuber extracts contained no amino acids. Terpenoids and saponins were found to be absent in *G. superba* shoot and flower extract (Jothi, et al. 2019).

In another study, phytochemical screening for aqueous and ethanolic extracts of *G. superba* tubers revealed the presence of alkaloids, flavonoids, and tannins in both solvents, as well as glycosides and saponins in the aqueous extract and phenols and terpenoids in the ethanolic extract, while steroids were absent in both extracts (Jayakumar, et al. 2018).

The presence of these secondary metabolites might be attributed to the traditional uses of the plant to treat various diseases such as microbial infections (Tulika and Pallavi 2020), leprosy, snake bite (Jana and Shekhawat 2011, Pulliah 2002), epilepsy (Belayneh and Bussa 2014), cancer (Ayele 2018) and gout and tumor (Solomon, et al. 2020).

Phytochemicals such as tannins, flavonoids, saponins, phenolic compounds, and essential oils are hypothesized to be responsible for plant antibacterial activities (Rahman et al., 2011). Flavonoids have been linked to numerous biological functions, including antibacterial, antioxidant, and anti-inflammatory properties. They are known to protect plants from illnesses (Hafidh et al., 2011; Dhiman et al., 2012). Tannins, flavonoids, alkaloids, and saponins have been shown to suppress pathogens by a synergistic action (Nwankwo et al., 2014). Therefore, the presence of these class of compounds in this plant confirms its potential for discovery of lead compounds that belong to these classes.

Table 3: Phytochemical screening tests on the root extract of *G. superba*

Secondary Metabolites	**Test**	**Solvents Used**		
		n-Hexane	Chloroform	Methanol
Alkaloids	Mayer's test	-	+	+
Flavonoids	Alkaline test	+	+	+
Glycosides	Salkowski's Test	+	+	+
Phenols	Ferric chloride test	+	+	+
Steroids	Salkowski's Test	+	+	+
Saponins	Froth Test	+	+	+
Tannins	Ferric chloride test	+	+	+
Terpenoids	Salkowski's Test	+	+	+

+ shows Presence - shows Absence

4.3 Characterization of Isolated Compounds

Compound **48** (14.4 mg) was isolated as white powder with R_f value of 0.3 (10% EtOAc in *n*-hexane as eluent). Its ^{1}H-NMR spectrum (400 MHz, $CDCl_3$) (**Appendix1**) revealed the existence of two aromatic protons with AB spin pattern at δ 6.94 (d, J = 8.0 Hz, 1H) and 7.09 (d, J = 8.1 Hz, 1H). Two oxygenated protons were observed at δ 3.95 (s, 3H) and 4.21 (t, J = 6.7 Hz, 2H) attributed to methoxy and oxygenated methylene, respectively. The presence of an olefinic proton signal at δ 6.31 (d, J = 15.9 Hz, 1H) and 7.63 (d, J = 15.9 Hz, 1H) were observed. Methylene and terminal methyl protons were observed at δ 1.71 (m, 2H), 1.61 (s, 2H), and δ 0.90 (t, J = 6.4 Hz, 3H), respectively.

The ^{13}C-NMR spectrum (100 MHz, $CDCl_3$) (**Appendix 2**) in combination with DEPT-135 (**Appendix 3**) displayed 17 carbon signals corresponding of which the peaks at δ_C 55.9 and δ_C 64.6 belong to methoxy and oxygenated methylene carbons whereas the peak δ_C14.1 suggests a terminal methyl group. Six methylene carbon signals were observed at δ_C64.6, 31.9, 29.4, 28.8, 26.0, and 22.7of which the first one is linked to heteroatom oxygen. The presence of two olefinic methine carbons was observed atδ_C114.7 and 144.6. Ester carbonyl carbon appeared at δ_C 167.4 whereas six aromatic carbons at δ_C147.9, 146.7,127.1,123.0, 117.6, and 115.7, of which peaks at δ_C127.1, 147.9, and 146.7 disappeared in DEPT-135, suggesting these peaks belong to quaternary carbons. The presence of the deshielded sp^2 methine (i.e., δ_C 144.6) suggests the presence of alpha beta conjugated system. Methylene signals pointed down in DPET-135 spectra, in good agreement with the ^{13}C NMR spectral data. The above spectral data suggest that the compound is 4-methoxy caffeic acid heptyl ester, isolated herein for the first time from the species.

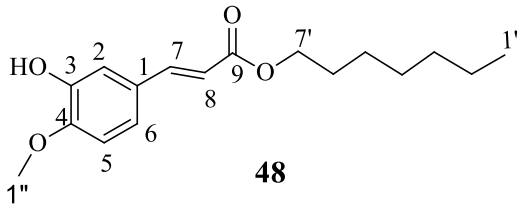

48

Figure 6: The structure of 4-methoxy caffeic acid heptyl ester (**48**)

Table 4: ^{1}H NMR and ^{13}C NMR data of compound **48**.

Carbon Position	^{1}H-NMR data of compound **48**	^{13}C-NMR data of compound **48**	^{1}H-NMR data of caffeoyl moiety*Takenaka et al. 2003*)	^{13}C-NMR data of caffeoyl moiety (*Takenaka et al. 2003*)	Types of carbons
1	-	127.1	-	127.87	C
2	7.09 (d, *J* = 8.1 Hz, 1H)	115.7	7.024 (d, J= 2.0 Hz)	115.27	CH
3	-	146.7	-	146.82	C-O
4	-	147.9	-	149.80	C-O
5	6.81 (d, J= 12.9 Hz)	117.6	6.758 (d, J = 8.3 Hz)	116.53	CH
6	6.94 (d, *J* = 8.0 Hz, 1H)	123.0	6.920 (dd J = 8.3 Hz)	123.26	CH
7	7.63 (d, J = 15.9 Hz, 1H)	144.6	7.529 (d J = 15.8 Hz)	147.97	= CH
8	6.31 (d, J = 15.9 Hz, 1H)	114.7	6.231 (d J = 15.8 Hz)	114.41	CH
9	-	167.4	-	167.77	Carbonyl carbon
1’	0.90 (t, *J* = 6.4 Hz, 3H))	14.1			CH_3
2’	1.71 (m, 2H)	22.7			CH_2
3’		31.9			CH_2
4’		28.8			CH_2
5’		26.0			CH_2
6’	1.61 (s, 2H)	29.4			CH_2
7’	4.21 (t, J = 6.7 Hz, 2H)	64.6			O-CH_2
1’’	3.95 (s, 3H)	55.9			O-CH_3

Compound **49** (14.2 mg) was isolated as pale-yellow powder with R_f value of 0.4 (20% EtOAc in *n*-hexane as eluent). The^{1}H NMR (400 MHz, $CDCl_3$) (**Appendix 4**) spectrum displayed signals of olefinic methine protons at δ 5.4 (brs, 1H) and 5.1 (brs, 1H), sp^3 oxygenated methine proton signal at δ 3.7 (m, H-3), and methylene proton adjacent to the oxygenated methine at δ 2.4. Five methyl signals of which four of them appeared as singlets at δ 0.7, 1.0, 1.6, and 1.9 confirming the methyl groups are attached to quaternary carbons, and one multiplate at δ 0.9.

The ^{13}C NMR (100 MHz, $CDCl_3$) (**Appendix 5**) spectrum displayed the presence of five methyl carbons which resonated at δ_C 11.9, 14.1, 19.4,19.8, and 22.7. Ten methylene carbon signals were observed resonating at δ_C 21.1, 24.3, 26.1, 28.3, 31.6, 33.7, 36.2, 36.5, 37.3 and 39.8. the presence of five methine carbons were observed at δ_C 31.9, 33.9, 50.1, 51.2, and 56.8. The peaks observed

at δ 42.3 and 45.8 in the ^{13}C NMR spectrum were sp^3 quaternary carbon atoms that belong to C-10 and C-13, respectively. The spectrum also showed sp^3 oxygenated methine at δ 71.8 (C-3) and olefinic carbons at δ 121.7 (C-6 and C-24), 132.2 (C-25), and140.7 (C-5) of which the latter belong to quaternary carbon. The above spectral data are in good agreement with data reported in the literature for desmosterol (Wilson, et al. 1996), reported herein for the first time from the species. Desmosterol is the immediate precursor of cholesterol in the Bloch pathway of cholesterol biosynthesis. 24-dehydrocholesterol reductase catalyzes the reduction of desmosterol to cholesterol.

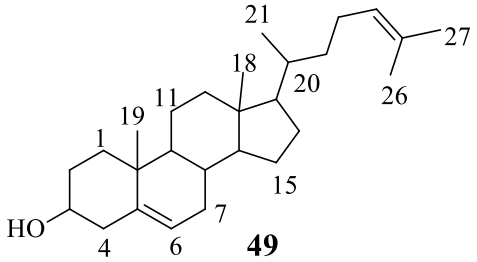

49

Figure 7: The structure of desmosterol (**49**)

Table 5: ^{1}H NMR and ^{13}C NMR data of compound **49**

Position	^{1}H-NMR data of compound **49**	^{13}C-NMR data of compound **49**	Reported^{1}H-NMR data of Desmosterol (Wilson *et al.* 1996)	Reported^{13}C-NMR data of Desmosterol (Wilson *et al*. 1996)	Types of carbons
1		36.5	1.078 ,1.845	37.2	CH_2
2		31.6	1.838, 1.500	31.6	CH_2
3	3.7 (s, 1H)	71.8	3.5	71.8	CH-O
4		42.3	2.294, 2.235	42.3	CH_2
5	-	140.7	-	140.7	C
6	5.4 (s, 1H)	121.7	5.4	121.7	= CH
7		33.7	1.529, 1.973	31.9	CH_2
8		31.9	1.454	31.8	CH
9	0.9 (m, 6H)	50.1	0.929	50.1	CH
10	-	37.3	-	36.5	C
11		21.1	1.50, 1.46	21.1	CH_2
12		39.8	1.158, 2.011	39.7	CH_2
13	-	45.8	-	42.3	C
14	0.9 (m, 6H)	56.8	0.989	56.7	CH
15		28.3	1.577,1.072	24.3	CH_2
16		26.1	1.839,1.266	28.2	CH_2
17		51.2	1.102	56.0	CH
18	0.7 (s, 3H)	11.9	0.680	11.8	CH_3

19	1.0 (s, 3H)	19.4	1.009	19.4	CH_3
20		33.9	1.396	35.6	CH
21	0.9 (m, 6H)	19.8	0.937	18.6	CH_3
22		36.2	1.408,1.041	36.1	CH_2
23	2.02 (s, 2H)	24.3	1.849,2.021	27.7	CH_2
24	5.1 (s, 1H)	121.7	5.1	125.2	= CH
25	-	132.2	-	130.9	C
26	1.9 (s, 3H)	22.7	1.682	25.7	CH_3
27	1.6 (s, 3H)	14.1	1.602	17.6	CH_3

Compound **50** (17.4 mg) was isolated as pale-yellow needleswith R_f value of 0.25 (20% EtOAc in *n*-hexane as eluent). Its ^{1}H-NMR spectrum (400 MHz, DMSO-d_6) (**Appendix6**) revealed the existence of ABX spin system aromatic protons at δ 7.0 (m, 2H), 7.3 (d, J = 7.4 Hz, 2H), and 6.8 (m, 2H). The presence of oxygenated methylene proton was displayed at δ 4.48 (d, J = 4.8 Hz, 2H).

The ^{13}C NMR spectrum (100 MHz, DMSO-d_6) (**Appendix 7**) in combination with DEPT-135 (**Appendix 8**) oxygenated methylene carbon signal at δ_C58.7 and six aromatic carbonsignals at δ_C115.0, 119.1, 127.8, 128.9, 144.3 and 154.6 of which the later suggest the presence of oxygenated sp^2 quaternary carbon. The above spectral data suggest that the compound is 3-(hydroxymethyl)phenol, reported herein for the first time from the plant. Previously of 3-(hydroxymethyl) phenol (**50**) was isolated from *Aspergillus nidulans*, and was demonstrated to possess significant biotechnological and pharmacological potential since it exhibited broad spectrum antimicrobial and anti-biofilm activities (Kumar *et al.*2017).

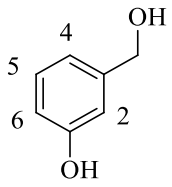

50

Figure 8: The structure of 3-(hydroxymethyl) phenol (**50)**

Table 6: ^{1}H NMR and ^{13}C NMR data of compound **50**

Position	^{1}H-NMR data of compound **50**	^{13}C-NMR data of compound **50**	Reported^{1}H-NMR data of compound **50** (Kumar *et al.*2017)	Reported^{13}C-NMR data of compound **50** (Kumar *et al.* 2017)	Types of Carbon
1	-	144.3	-	142.66	C
2	7.0 (m, 1H)	119.1	6.86 (br, s)	119.07	CH
3	-	154.6	-	155.95	C-O
4	6.8 (m, 1H)	127.8	6.89 (1H, dd, J = 7.3 & 1.5)	144.62	CH
5	7.3 (d, *J* = 7.4 Hz, 1H)	128.9	7.22 (1H, dd, J = 7.3 & 7.2)	129.83	CH
6	6.8 (m, 1H)	115.0	6.75 (1H, dd, J = 7.2 & 1.5)	113.77	CH
1’	4.48 (d, *J* = 4.8 Hz, 2H)	58.7	4.65 (2H, s)	65.07	CH_2-O

Compound **51**(12.8 mg) was isolated as pale-yellow needles with R_f value of 0.25 (30% EtOAc in *n*-hexane as eluent). Its ^{1}H-NMR spectrum (400 MHz, DMSO-d_6) (**Appendix9**) revealed the existence of three aromatic protons at δ 7.20 (d, J = 8.2 Hz, 1H) and 6.49 (d, J = 14.3 Hz, 2H) suggesting a trisubstituted aromatic ring. The presence of methoxy group was observed at δ3.7 (s, 3H).

The ^{13}C NMR spectrum (100 MHz, DMSO-d_6) (**Appendix 10**) in combination with DEPT-135 (**Appendix 11**) displayed eight carbon signals of which the presence of carboxyl carbonyl, and two sp2 oxygenated quaternary carbons were observed at δ_C 169.0, δ_C 157.3, and 158.1, respectively. Methoxy carbon was also evident at δ_C 56.2. Three sp2 methines were evident at δ_C 102.6, 109.2, and 110.8 whereas sp^2 quaternary carbon appeared at δ_C131.9. The disappearance of peaks at δ_C 169.0, δ_C 157.3, 158.1 and δ_C 131.9 complement these carbons are quaternary carbons. The above spectral data suggest that the compound is 3-Hydroxy-5-methoxy-benzoic acid (**51**), reported herein for the first time from the plant.

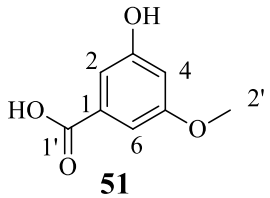

51

Figure 9: The structure of 3-Hydroxy-5-methoxy-benzoic acid (**51**)

Table 7: ^{1}H NMR and ^{13}C NMR data of compound **51**

Position	^{1}H-NMR data of compound **51**	^{13}C-NMR data of compound **51**	Reported ^{1}HNMR data of compound **51** *(Legrand et al. 2004)*	Reported ^{13}C-NMR data of compound **51** *(Legrand et al. 2004)*	Type of carbons
1'		169.0		165.95	Carbonyl
1	-	131.9	-	131.35	C
2	6.49 (d, *J* = 14.3 Hz, 1H)	110.8	6.91 (s, 1 H	105.99	CH
3	-	158.1	-	160.35	C
4	7.20 (d, *J* = 8.2 Hz, 1H)	102.8	6.97 (s, 1 H	104.99	CH
5	-	157.3	-	158.53	C
6	6.49 (d, *J* = 14.3 Hz, 1H)	109.2	6.58 (s, 1 H	108.54	CH
2'	3.7 (s, 3H)	56.2	3.82 (s, 3 H)	55.15	CH_3-O

Compound **52** (100.8 mg) was isolated as white powder with R_f value of 0.65 (20% MeOH in DCM as eluent). Its ^{1}H-NMR spectrum (400 MHz, DMSO-d_6) (**Appendix12**) revealed anomeric proton at δ 5.2 (d, J = 3.8 Hz, 1H). Oxygenated methylene was observed at δ 4.9 (s, 2H).

The ^{13}C NMR spectrum (100 MHz, DMSO-d_6) (**Appendix 13**) in combination with DEPT-135 (**Appendix 14**) displayed twelve carbon signals corresponding to two methylene carbon signals resonating at δ_C 60.9and 62.5, and anomeric carbon signals resonating at δ_C104.5 and 92.2. Carbon bearing a hydroxy functional group were also apparent from δ_C 70.3 to 82.9. DEPT-135 spectra displayed peaks at δ_C 62.6 and 60.9 pointing down in good agreement with the presence of two oxygenated methylene carbons. The above spectral evidence supports the compound is a disaccharide sugar composed of glucose and fructose subunits. Thus, based on the spectral data the compound was identified as sucrose. Previously, sucrose crystals were grown using the isolated from the hot MeOH extract of the rhizome powder of *G. superba* (Gopinath et al. 2015).

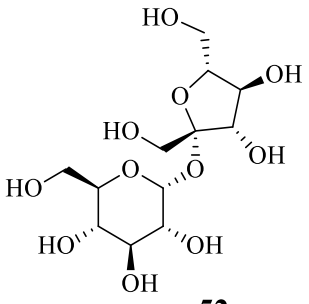

52

Figure 10: The structure of sucrose (**52**)

Table 8: ^{1}H NMR and ^{13}C NMR data of compound **52**

Position	^{1}H-NMR of Compound **52**	^{13}C-NMR data of Compound **52**	^{13}C-NMR data of sucrose *(Gopinath et al. 2015)*
1	5.2 (d, J = 3.8 Hz, 1H)	92.2	92.18
2	3.74 (s, 1H)	72.1	72.07
3	3.49 (m, 2H)	73.3	73.26
4	3.4 (s, 2H)	70.3	70.27
5	3.74 (s, 1H)	73.3	73.26
6	3.5 (t, *J* = 9.4 Hz, 1H) 3.2 (s, 3H)	60.9	60.91
1’	3.9 (d, *J* = 8.2 Hz, 1H)	62.5	62.57
2’	3.21 (d, *J* = 3.6 Hz, 3H)	104.5	104.47
3’	3.8 (m, 1H)	77.5	77.43
4’	4.9 (s, 2H)	74.7	74.70
5’	3.6 (m, 1H)	82.9	83.00
6’		62.5	62.47

Compound **53** (169.3 mg) was isolated as reddish-brown powder with R_f value of 0.62 (20% MeOH in DCM as eluent). Its ^{1}H-NMR spectrum (400 MHz, DMSO-d_6) (**Appendix15**) exhibited two doublets 5.2 (d, J = 3.7 Hz, 1H) and 3.9 (d, *J* = 8.2 Hz, 1H) that are assigned for the anomeric protons of the glucose, H-1and rhamnose H-1’ moieties, respectively. The latter signal along with the multiplate observed at δ 1.3 (m, 3H) for a secondary methyl group was evident for the presence of rhamnopyranose moiety. The spectrum also exhibited a series of peaks in the region between 4.00-3.00 accounting for the presence of oxygenated methine protons.

The ^{13}C NMR spectrum (100 MHz, DMSO-d_6) (**Appendix 16**) in combination with DEPT-135 (**Appendix 17**) displayed twelve carbon signals of which two anomeric carbons and oxygenated methylene appeared at δ104.3 (C-1'), 92.2 (C-1) and δ_C60.8, respectively. Oxygenated methines carbons were evident in between δ 77.5 to 62.5. Moreover, a methyl signal was observed δ17.9. The above spectral evidence supports a disaccharide sugar containing a rhamnose and glucose subunits. Thus, based on the above spectral data the compound was identified as6-O-α-L-rhamnosyl-D-glucose (rutinose, **53**).

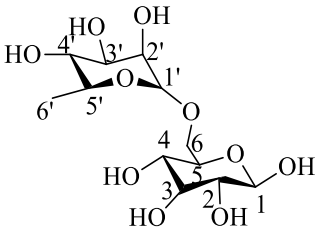

53

Figure 11: The structure of rutinose or**6**-O-α-L-rhamnosyl-D-glucose

Table 9: ^{1}H NMR and ^{13}C NMR data of compound **53**.

Position	^{1}H-NMR data of Compound **53**	^{13}C-NMR data of Compound **53**	Reported ^{13}C-NMR data of rutinose *(Neszmelyi et al. 1978)*
1	5.2 (d, J = 3.7 Hz, 1H)	92.2	91.9
2	3.2 (d, *J* = 3.6 Hz, 3H)	80.7	70.7
3	3.5 (t, *J* = 9.4 Hz, 3H)	73.2	72.9
4		62.5	68.9
5		70.2	72.9
6	3.2 (s, 3H)	60.8	61.8
1'	3.9 (d, *J* = 8.2 Hz, 1H)	104.3	98.8
2'		75.3	69.4
3'	3.4(s, 2H)	71.9	70.0
4'	3.6 (m, 1H)	74.6	71.3
5'	4.2 (s, 1H)	77.5	66.4
6'	1.3 (m, 3H)	17.2	17.5

4.4 Antibacterial Activity

The antibacterial activity of crude extracts and isolated compounds was evaluated by measuring the size of the zone of inhibition against the test organisms (**Table 10 and 11**). The results revealed that the extracts displayed promising growth inhibitory effect at the concentration of 200 mg/mL against the selected bacterial strains. The *n*-hexane extract showed highest zone of inhibition (13.33±0.58 mm) against *E. coli*, followed by inhibition against *S. typhimurium* and *K. pneumoniae* with the zone of inhibition values of12.67±0.58 and 11.0±1.00 mm, respectively. The finding is promising in comparison to the standard drug (gentamicin). The drug showed inhibition zones of 26.71±2.36, 28.86±2.34, and 21.67±2.55 mm against *E. coli*, *S. typhimurium* and *K. pneumoniae*, respectively. Similarly, the chloroform extract exhibited growth inhibition effect against *K. pneumoniae, S. typhimurium, S. aureus,* and *E. coli* with mean inhibition zones of 13.00±0.00, 13.00±1.00, 12.33±0.58and 12.00±1.00 mm, respectively. The MeOH extract was also found to be the only one active against *P. aeruginosa* (11.33±0.58 mm) and *E. faecalis* (12.00±0.0 mm) at higher concentration but inactive in lower concentrations. The extract also displayed activity against *E. coli* (11.67±1.15 mm) and *K. pneumoniae* (10.00±1.00 mm). In comparison to the *n*-hexane and MeOH extract, (at smaller concentration of 25 mg/mL) the chloroform extract showed the highest mean inhibition zone of (11.00±0.00 mm) against *K. pneumoniae* and (10.67±0.58 mm) against *S. typhimurium* and*E. Coli* (**Table 10**).

According to Megala and Elango (2012) *G. superba* tuber and seed extracts showed appreciable antibacterial effect against the tested *E. coli, K. pneumoniae, P. mirabilis, P. aeruginosa, and S. aureus*. The results showed that the dichloromethane extract exhibited pronounced inhibition against all the tested organisms. The maximum inhibition was observed on *P. mirabilis* in dichloromethane tuber extract 16 mm and *E. coli* in methanol tuber extract 15 mm and *S. aureus* in methanol tuber extract 15 mm. *K. pneumoniae* was found to be moderately suppressed by methanol tuber extract 14 mm and acetone seed extract 14 mm followed by *P. aeruginosa* methanol seed extract 14 mm compared to the positive control, streptomycin (Megala and Elango, 2012).

These activities can be due to the potential ability of the secondary metabolites to shape a complex with extracellular proteins and with the cell wall of microorganism. The higher inhibition effect of the extracts might be due to better solubility of those secondary metabolites, which showed the presence of a wide spectrum of antibiotic compounds (Jothi, et al. 2019). Therefore, phytochemical compounds are abundant in many plant elements for herbal protection against microbial illness. In

tuber extracts, phytochemical examination revealed the presence of alkaloids, flavonoids, terpenoids, tannins, saponins, phenolic compounds, glycosides and steroids (**Table 3**). As a result, phytochemical compounds may be responsible for *G. superba's* bacterial activity.

Table 10: Antibacterial activity of *G. superba* root extracts against selected bacterial strains

Extract	Conc (mg/ml)	Inhibition Diameter (mm)±SD					
		E. coli	*P. aeruginosa*	*K. pneumoniae*	*E. faecalis*	*S. typhimurium*	*S. aureus*
***n*-Hexane**	200	13.33±0.58	NE	11±1.0	NE	12.67±0.58	NE
	100	13.33±0.58	NE	10.33±1.15	NE	10.67±0.58	NE
	50	12±1.00	NE	9.33±1.15	NE	9.67±0.58	NE
	25	10.67±1.53	NE	9±1.73	NE	9.33±1.15	NE
Chloroform	200	12±1.00	NE	13±0.00	NE	13±1.00	12.33±0.58
	100	12±1.00	NE	12.33±0.58	NE	12±1.00	NE
	50	10.67±0.58	NE	11.67±0.58	NE	11.67±0.58	NE
	25	8.33±1.53	NE	11±0.00	NE	10.67±0.58	NE
Methanol	200	11.67±1.15	11.33±0.58	10±1.00	12±0.00	NE	NE
	100	11±1.00	10±1.00	10±1.00	NE	NE	NE
	50	11±1.00	NE	11.33±0.58	NE	NE	NE
	25	8.33±2.08	NE	8±0.00	NE	NE	NE
Gentamycin	100	26.71±2.36	25±2.52	15.86±4.67	NE	28.86±2.34	25.43±2.15

NE= No Effect

Similar experiments on the isolated compounds showed antibacterial activity *in vitro* with mean inhibition zones displayed in the range between 6.67 and 15.00 mm for tested bacterial strains (**Table 11**). Among the isolated compounds, the *in vitro* antibacterial activity displayed by compound **50** showed highest activity both at higher and lower concentrations (15.00±0.00 and 11.00±0.00 mm at 1 mg/mL and 125 µg/mL respectively) against *S. typhimurium* compared to gentamicin (28.86±2.34mm at 100 µg/mL).

Compounds**49**and **51** showed relatively strong antibacterial activity (14.00±1.00 and 14.00±1.73 mm at 1 mg/mL) against *P. aeruginosa* compared to gentamicin (25.00±2.52 mm at 100 µg/mL) while the others did not show activity (**Table 11**).

Compounds **49, 50,** and **51**displayed comparable activity (11.33±1.53, 10.00±1.73, and 11.67±1.15mm, respectively at 500 µg/mL) against *K. pneumoniae* compared to gentamicin (15.86±4.67mm at 100 µg/mL) while compound **51** showed higher activity (13±1.00mm at 1

mg/mL) against *E. coli*, and the only one active against *E. faecalis* (12.33±0.58mm at 100 µg/mL) (**Table 11**).

Table 11:The antibacterial activities of isolated compounds, **48-51** against selected bacterial strains

Compound	Conc (µg/ml)	Inhibition Diameter (mm)±SD					
		E. coli	*P. aeruginosa*	*K. pneumoniae*	*E. faecalis*	*S. typhimurium*	*S. aureus*
48	500	11.33±0.58	NE	NE	NE	10.33±0.58	NE
	250	10±1.00	NE	NE	NE	9.33±0.58	NE
	125	10±0.00	NE	NE	NE	8.33±0.58	NE
	62.5	8.33±0.58	NE	NE	NE	7.33±0.58	NE
49	1000	10.67±1.15	14±1.00	12.33±0.58	NE	15±0.00	12.67±1.15
	500	10±1.73	13.67±0.58	11.67±1.15	NE	14±2.00	12.33±1.15
	250	8.33±2.52	12±1.00	11.33±1.53	NE	11.33±0.58	12±.00
	125	7.67±2.89	10.67±0.58	10.33±0.58	NE	11±0.00	9.33±2.08
50	500	NE	NE	11.33±1.53	NE	8.33±0.58	NE
	250	NE	NE	10±1.00	NE	7.33±1.15	NE
	125	NE	NE	9±1.00	NE	NE	NE
	62.5	NE	NE	7.33±0.58	NE	NE	NE
51	1000	13±1.00	14±1.73	11.33±1.15	12.33±0.58	11.33±0.58	10.67±0.58
	500	11.67±0.58	12.33±1.53	10±1.73	11.33±0.58	10±0.00	9.67±0.58
	250	10.66±1.15	10.67±0.58	9.67±1.53	8.67±2.31	8.67±0.58	7±0.00
	125	NE	10±1.00	7±1.00	7±1.00	8±0.00	NE
Gentamycin	100	26.71±2.36	25±2.52	15.86±4.67	NE	28.86±2.34	25.43±2.15

NE= No Effect

4.5 Antioxidant Activity

Multiple techniques can be used to test antioxidant activity in vitro and in vivo. Because of its simplicity, speed, and low cost, the DPPH-based technique is likely the most widely used in vitro assay (Alam et al., 2013). The stable free radical DPPH (1,1-diphenyl-2-picrylhydrazyl) can be decreased by transferring hydrogen from other molecules. In the DPPH antioxidant assay, the ability of DPPH to decolorize in the presence of antioxidants is employed. The deep purple color is caused by the odd electron in the DPPH radical. DPPH decolorizes when it accepts an electron from an antioxidant molecule (Kumarasamy et al., 2007).

The DPPH scavenging assay of crude extracts of *G. superba* was tested for the free radical scavenging ability by interaction with stable DPPH radicals. The reduction of DPPH was accompanied by a decrease in absorbance at 517 nm. The DPPH was greatly reduced by the crude

extracts, especially by the chloroform extract. At a concentration of 200 µg/ml, the DPPH radical scavenging activities (%) were found to be 27.11, 72.98, and 95.14 for *n*-hexane, methanol, and chloroform extracts, respectively (**Table 12** and **Figure12**).

The DPPH radical scavenging activity (%) of aqueous, ethanolic, and benzene extracts of *G. superba* tubers were reported to be65.575±0.183, 91.786±0.050, and 55.939±0.154, respectively, in the study of Jayakumar, et al. (2018) at a concentration of 200 g/ml (Jayakumar, et al. 2018). Also, in another study different concentrations of methanolic extracts at100 µg of *G. superba* whole plant parts such as shoot, flower, tuber showed a radical scavenging 65.76µg/ml, 60.34 µg/ml, 80.12 µg/ml, respectively.

The DPPH scavenging activities were found to decrease as the concentration of the samples in the assay got reduced. The positive control (ascorbic acid) showed a maximum scavenging effect at very low and high concentrations (88.63% - 96.11%). The IC_{50} value is a parameter widely used to measure the antioxidant activity of test samples. It is calculated as the concentration of antioxidants needed to decrease the initial DPPH concentration by 50%. Thus, low IC_{50} values correspond to a higher antioxidant capacity (Fausto *et al*., 2020). Compared to the standard ascorbic acid, the DPPH radical scavenging activities of the extracts were found to be lower except for the chloroform extract that has showed comparable activity with lower IC_{50} value (5 µg/mL) which corresponds to its strong antioxidant activity.

Table 12: DPPH radical scavenging activities (%) of *G. superba* root extract

Conc (µg/ml)	**Control**	**Extracts**						**Positive control**	
		Hexane		Chloroform		Methanol		Ascorbic Acid	
		A	%RSA	A	%RSA	A	%RSA	A	%RSA
200	1.029	0.75	27.11	0.05	95.14	0.278	72.98	0.04	96.11
100	1.029	0.831	19.24	0.134	86.98	0.543	47.23	0.045	93.68
50	1.029	0.852	17.20	0.247	75.996	0.67	34.89	0.047	90.57
25	1.029	0.854	17.01	0.314	69.48	0.8	22.25	0.05	88.63
IC_{50}		424.3		5.7		110		0.0007	

A- Absorbance, RSA-Radical Scavenging Activity, IC_{50} – 50% Inhibitory Concentration

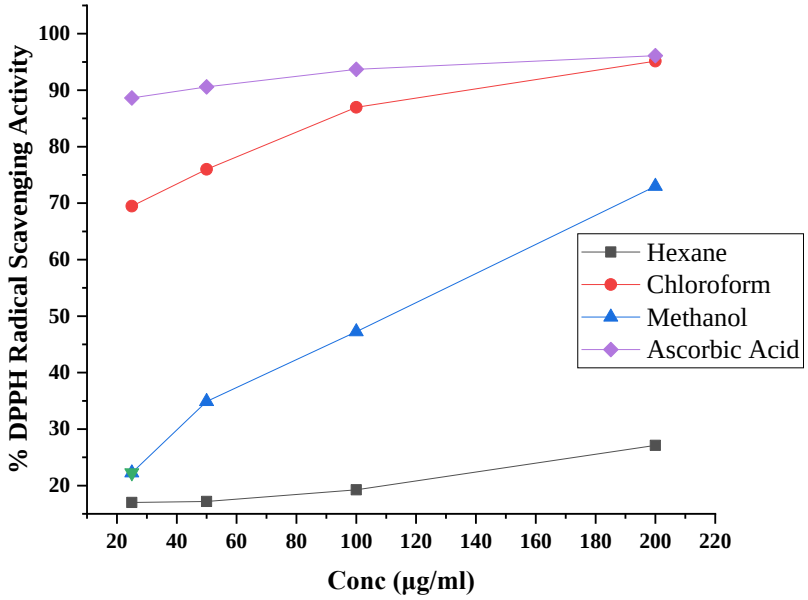

Figure 12:% Inhibition of the extracts and the standard drug at the different concentration ranges

The percent DPPH radical scavenging activities of isolated compounds were found to be 33.57,35.69, 28.86 and 23.14 for compounds **48, 49**, **50**and **51,** respectively (**Table 13** and **Figure 13**). For the various concentrations, compounds **48**and **49** exhibited higher percent inhibition as compared to the rest of isolated compounds (**50** and **51**). When compared to the standard ascorbic acid, the DPPH radical scavenging activities of isolated compounds were generally found to lower than the standard compound (**Table 13**).

Table 13: DPPH radical scavenging activities (%) of isolated compounds **48-51**

Conc (µg/ml)	**Control**	**Compounds**								**Positive Control**	
		48		**49**		**50**		**51**		Ascorbic Acid	
		A	%RSA	A	%RSA	A	%RSA	A	%RSA	A	%RSA
20	1.275	0.847	33.57	0.82	35.69	0.907	28.86	0.98	23.14	0.028	97.80
10	1.275	0.91	28.63	0.872	31.61	0.972	23.76	1.019	20.08	0.045	96.47
5	1.275	0.954	25.18	0.875	31.37	0.985	22.75	1.033	18.98	0.573	55.06
2.5	1.275	0.973	23.69	0.89	30.196	1.076	15.61	1.094	14.196	0.875	31.37
IC_{50}		50		40		140		600		4	

A- Absorbance, RSA-Radical Scavenging Activity, IC_{50} – 50% Inhibitory Concentration

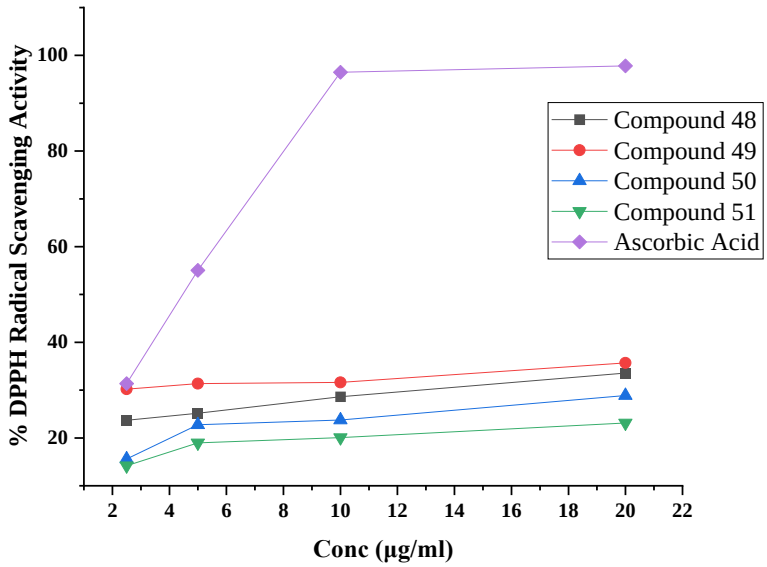

Figure 13: % Inhibition of the isolated compounds and the standard drug at the different concentration ranges

4.6 *In silico* Molecular Docking Study

Molecular docking was considered a powerful computational technique in structure-based drug development because it allowed the prediction of protein-ligand binding interactions of new molecules at suitable target binding sites and explained the associated inhibitory effect of binding affinity, H-bond, hydrophobic, and Van der Waals interactions of ligands (**Tables 14-17**). The majority of the target products have promising docking scores and interactions with various amino acid residues (2D and 3D), as shown in **Figure 14-33**. The structure of the target protein binding pocket is depicted as a ribbon model, with hydrogen bonds between compounds and amino acids indicated by green dotted lines and hydrophobic interactions indicated by pink lines.

The molecular docking study was carried out to assess the binding affinities and binding interactions of isolated compounds **48-51**with target proteins *E.coli*, DNAgyrase B (PDB ID: 6F86), *S. aureus*, Pyruvate Kinase (PDB ID: 3T07), *P. aeruginosa*, PqsA (PDB ID: 5OE3), and Human Peroxiredoxin 5 (PDB ID: 1HD2).The binding affinity, amino acid residues that are involved in hydrogen bonds, hydrophobic, and van der Waals interactions at each ligand- protein complexes were mapped using AutoDock Vina (**Figure 14-33**, and **Tables 14-17**).

The docked compounds **49-51** displayed minimum binding energies ranged from -5.2 to - 6.7 kcal/mol, -3.4to -4.7 kcal/mol, -6.3 to -7.8 kcal/mol, and -4.2 to -4.9 kcal/mol with DNA gyrase B, Pyruvate Kinase, PqsA, and Human Peroxiredoxin 5, respectively (**Tables 14-17**). Such low docking score values signify good interactions of the compounds with protein binding pocket.

In the study, each of the isolated compounds (**49-51**) demonstrated comparable to better binding affinity (binding energy of – 6.7 to - 5.2 kcal/mol) against protein DNA gyrase than the standard drug, amoxicillin (− 6.1 kcal/mol). The highest binding affinity (− 6.7 kcal/mol) was recorded by compound **49** followed by compound **51** (− 5.7 kcal/mol).

All the compounds have showed hydrogen bonding interactions. Compound **49** showed H-bonding interaction with amino acid residues Asn-46, compound **50** showed interaction with Thr-165 and compound **51** showed interaction with Gly-77, Asp-73, and Thr-165 as showed in **Table 14** below. All the compounds except compound **49** exhibited more residual Van der Waals interaction than the standard drug amoxicillin.

Table 14: Molecular docking value of isolated compounds (**49-51**) against DNA gyrase B (PDB ID: 6F86)

Compounds	**Affinity (kcal/mol)**	**H-bond**	**Residual interactions**	
			Hydrophobic	Van der Waals interaction
49	-6.7	Asn-46	Arg-76, Ile-78, Pro-79	Ala-47, Asp-73, Thr-165, Glu-50, Gly-77, Arg-136
50	-5.2	Thr-165	Gly-77, Glu-50, Ile-78	Arg-76, Gly-75
51	-5.7	Gly-77, Thr-165, Asp-73	Glu-50, Ile-78	Ile-94, Pro-79, Arg-76, Gly-75, Ala-47
Amoxicillin	-6.1	Asp-73, Arg-76, Asn-76, Gly-77	Pro-79	Ile-94, Thr-165, Arg-136

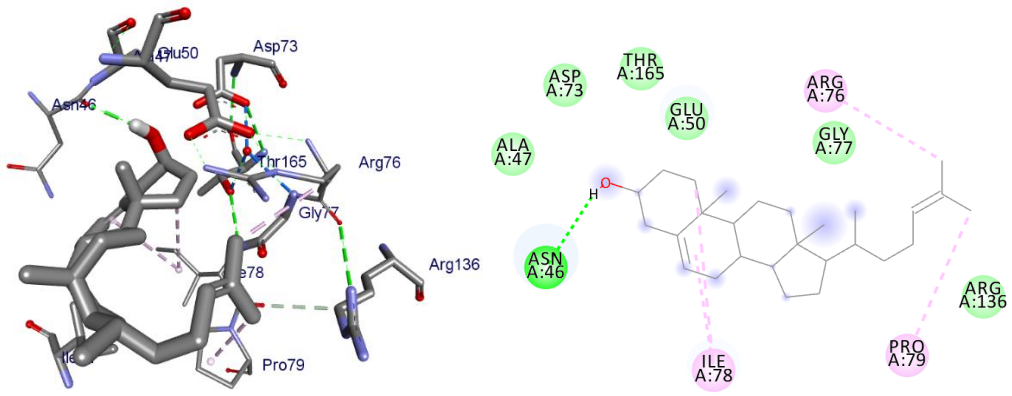

Figure 14: 3D (b) and 2D (a) representations of the binding interactions of compound **49** against *E. coli* DNA Gyrase B (PDB ID: 6F86).

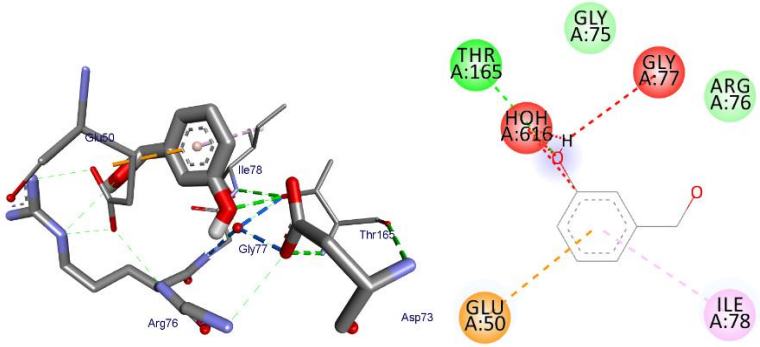

Figure 15: 3D (b) and 2D (a) representations of the binding interactions of compound **50** against *E. coli* DNA Gyrase B (PDB ID: 6F86).

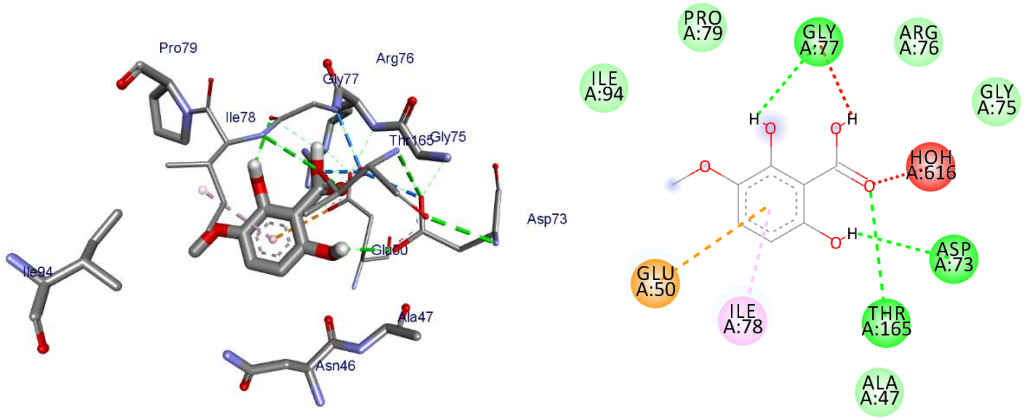

Figure 16: 3D (b) and 2D (a) representations of the binding interactions of compound **51** against *E. coli* DNA Gyrase B (PDB ID: 6F86).

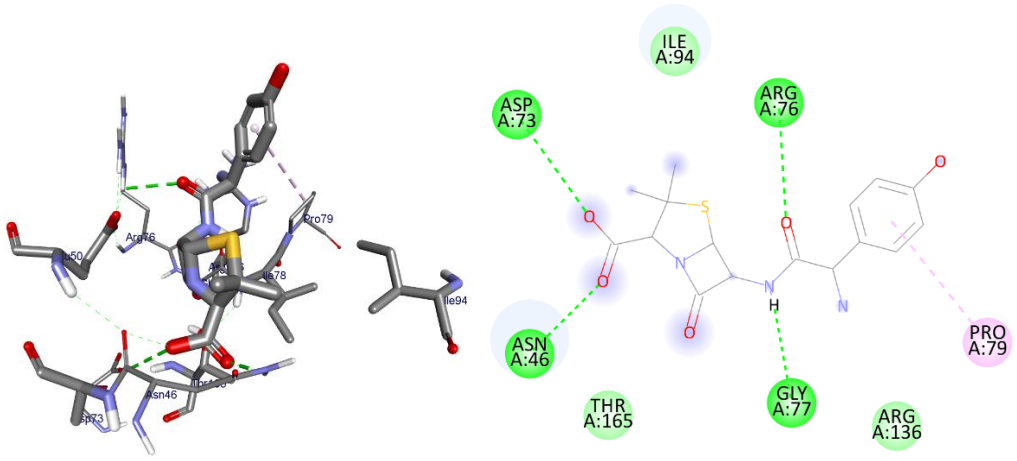

Figure 17: 3D (b) and 2D (a) representations of the binding interactions of amoxicillin drug against *E. coli* DNA Gyrase B (PDB ID: 6F86).

The binding affinities of the ligands (**49-51**) to the protein Pyruvate Kinase (-3.4 to -4.7 kcal/mol) were found to be equal to or less than amoxicillin (-4.7 kcal/mol). Of these, the strongest binding affinity was displayed by compound **49** (-4.7 kcal/mol). Compounds **49** and **51**showed H-bonding interaction. Compound **49** showed H-bonding interaction with amino acid Thr-353 and Thr-348, and compound **51** showed interaction with Ala-358 (**Table 15).**

Table 15: Molecular docking value of isolated compounds (**49-51**) against Pyruvate Kinase (PDB ID: 3T07)

Compounds	**Affinity (kcal/mol)**	**H-bond**	**Residual interactions**	
			Hydrophobic	Van der Waals interaction
49	-4.7	Thr-353, Thr-348	Ala-358, Ile-361	Lys-349, Ser-362, Ser-354
50	-3.4	-	Ala-358, Ile-361	Thr-353, Ser-354, Ser-362
51	-3.4	Ala-358	Ile-361	Ile-359, Thr-353, Ser-354
Amoxicillin	-4.7	Thr-464, Thr-463, Leu-355, Ala-358	Ala-358, Ile-359	Ser-361, Ser-362

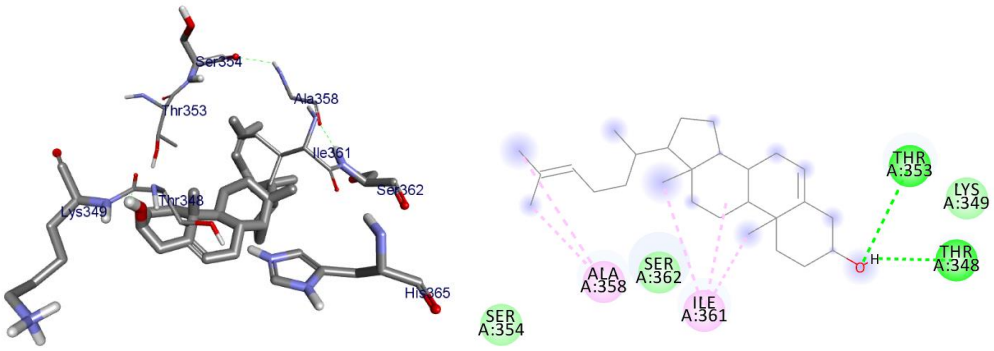

Figure 18: 3D (b) and 2D (a) representations of the binding interactions of compound **49** against *S. aureus* Pyruvate Kinase (PDB ID: 3T07).

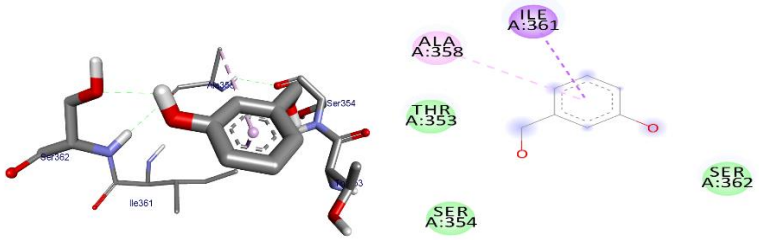

Figure 19: 3D (b) and 2D (a) representations of the binding interactions of compound **50** against *S. aureus* Pyruvate Kinase (PDB ID: 3T07).

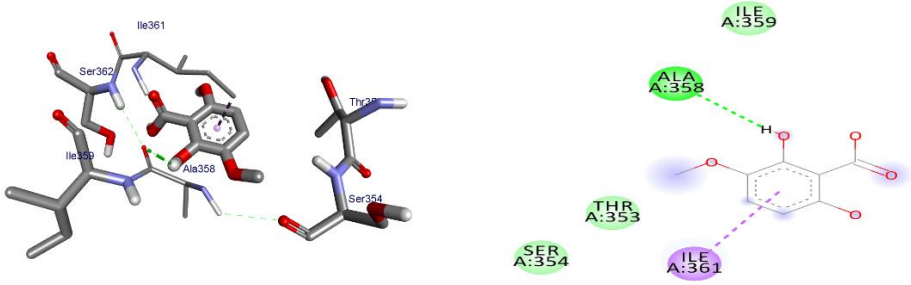

Figure 20: 3D (b) and 2D (a) representations of the binding interactions of compound **51** against *S. aureus* Pyruvate Kinase (PDB ID: 3T07).

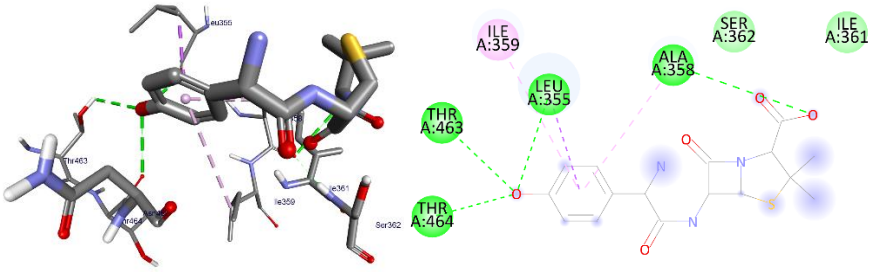

Figure 21: 3D (b) and 2D (a) representations of the binding interactions of compound amoxicillin against *S. aureus* Pyruvate Kinase (PDB ID: 3T07).

When docked to the protein PqsA, compound **49** displayed higher binding affinity (-7.8 kcal/mol) as compared to the standard drug, amoxicillin (-7.3 kcal/mol). The rest of the compounds showed that the binding affinities to be lower than the standard drug. In the interaction with PqsA, compound **51**displayed H-bonding interactions with amino acid Thr-304 and Ala-303, respectively (**Table 16**).

Table 16: Molecular docking value of isolated compounds (**49-51**) against PqsA (PDB ID: 5OE3)

Compounds	**Affinity (kcal/mol)**	**H-bond**	**Residual interactions**	
			Hydrophobic	Van der Waals interaction
49	-7.8	-	Ser-280, Pro-281, His-394, Ile-301, Phe-209, Tyr-211, Arg-397, Ala-303	Asp-382, Gly-302, Gly-210, Thr-304, Gly-279
50	-6.3	-	Gly-279, His-308, Tyr-211, Ala-278, Gly-210, Gly-302	Gly-300, Phe-209, Ala-303, Thr-304, Gly-307, Val-309
51	-6.5	Ala-303	Gly-279, Gly-302, Ala-278, Phe-209, Tyr-211	Val-309, Gly-210, Thr-304
Amoxicillin	-7.3	Glu-305, Asp-299, Thr-323, Gly-279, Gly-302	Ile-301, Pro-281, Ser-280, Asp-382	Tyr-378, Thr-380, Arg-378, Gly-300, Leu-282

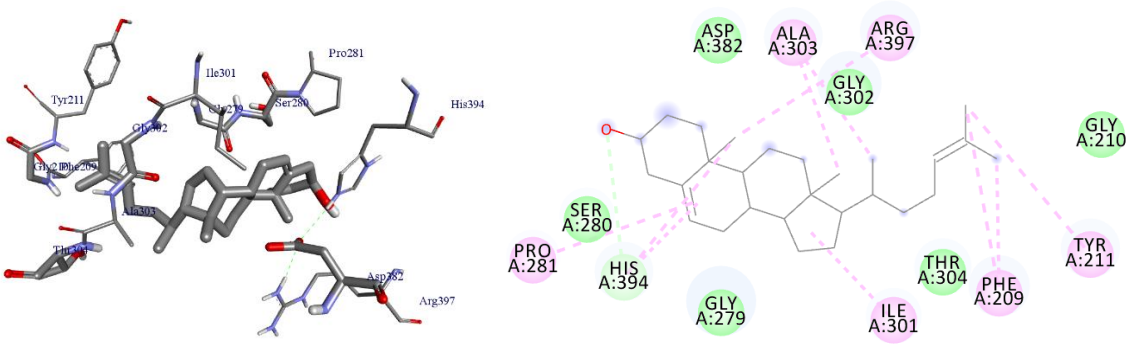

Figure 22: 3D (b) and 2D (a) representations of the binding interactions of compound **49** against *P. aeruginosa* PqsA (PDB ID: 5OE3).

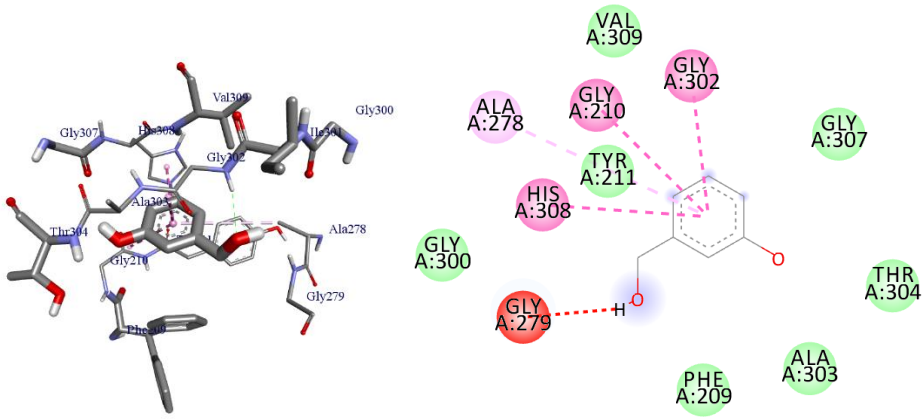

Figure 23: 3D (b) and 2D (a) representations of the binding interactions of compound **50** against *P. aeruginosa* PqsA (PDB ID: 5OE3).

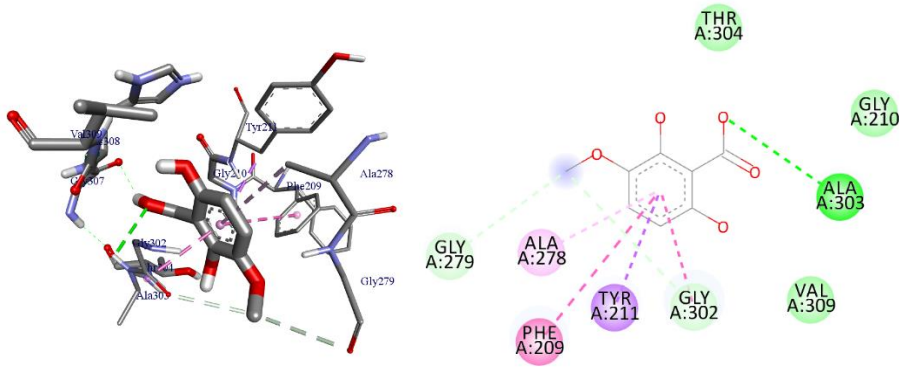

Figure 24: 3D (b) and 2D (a) representations of the binding interactions of compound **51** against *P. aeruginosa* PqsA (PDB ID: 5OE3).

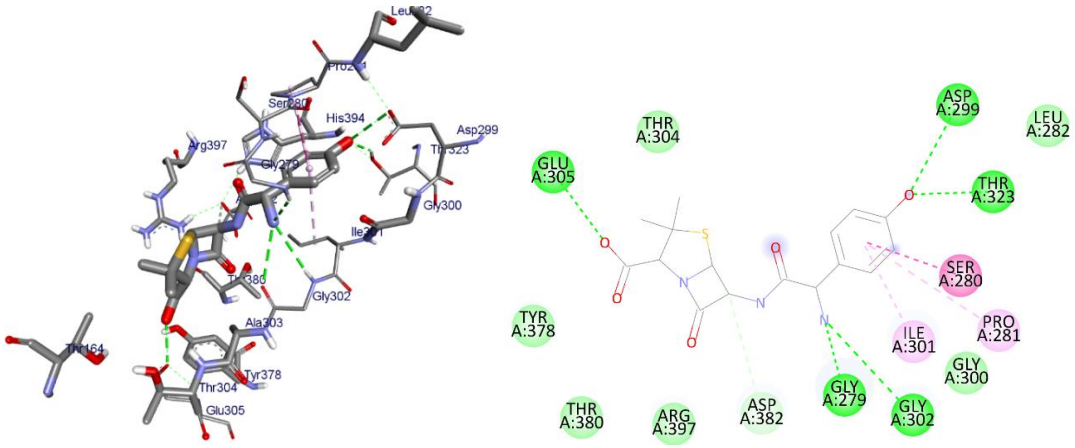

Figure 25: 3D (b) and 2D (a) representations of the binding interactions of amoxicillin against *P. aeruginosa* PqsA (PDB ID: 5OE3).

The isolated compounds (**49-51**) were found to have minimum binding energy ranging from -4.98 to -6.3 kcal/mol against the Human Peroxiredoxin 5 (**Table 17**). From these, the best result was achieved using compound **49** (-6.3 kcal/mol). The compounds **50** and **51** showed H-bonding interactions. Compound **50** showed interaction with Cys-47, Thr-147, and compound **51** showed interaction with Thr-147, Gly-46 and Thr-44 (**Table 17**).

Table 17: Molecular docking value of the isolated compounds (**49-51**) against Human Peroxiredoxin 5 (PDB ID:1HD2)

Compounds	Affinity (kcal/mol)	H-bond	Residual interactions	
			Hydrophobic	Van der Waals interaction
49	-4.6	-	Pro-40, Pro-45, Phe-120, Leu-116, Leu-149	Asp-145, Gly-46, Arg-127, Gly-148
50	-4.2	Cys-47, Thr-147	Arg-127, Pro-40	Pro-45, Thr-44, Phe-120, Gly-148
51	-4.9	Thr-147, Gly-46, Thr-44	Pro-40, Arg-127	Leu-116, Leu-149, Cys-47, Pro-45
Amoxicillin		Arg-127, Thr-147, Gly-46	Ile-119, Phe-120	Thr-44, Cys-47, Leu-149, Pro-45

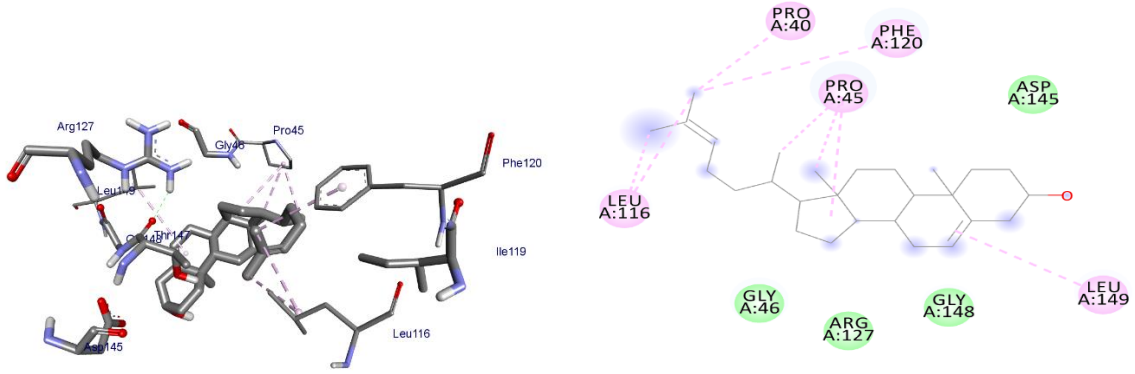

Figure 26: 3D (b) and 2D (a) representations of the binding interactions of compound **49** against human peroxiredoxin 5 (PDB ID: 1HD2).

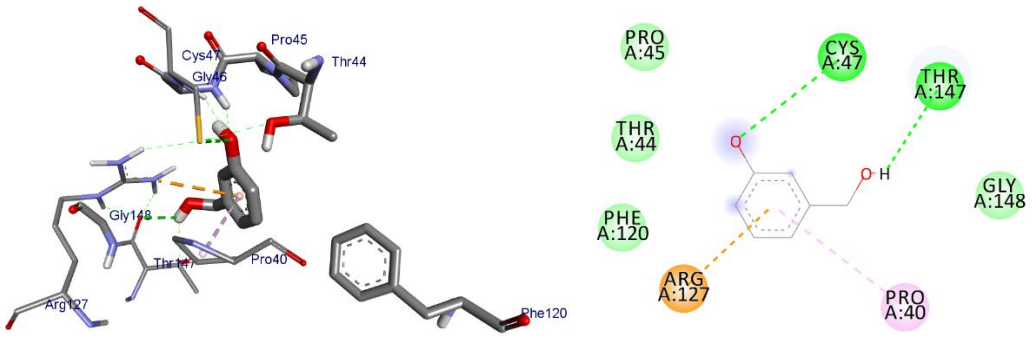

Figure 27: 3D (b) and 2D (a) representations of the binding interactions of compound **50** against human peroxiredoxin 5 (PDB ID: 1HD2).

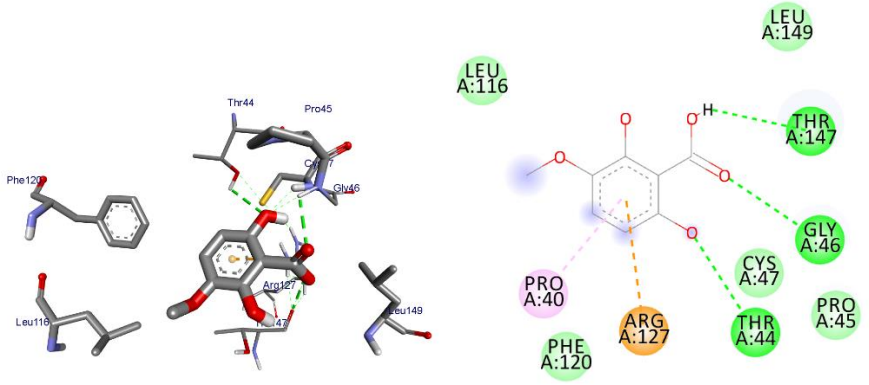

Figure 28: 3D (b) and 2D (a) representations of the binding interactions of compound **51** against human peroxiredoxin 5 (PDB ID: 1HD2).

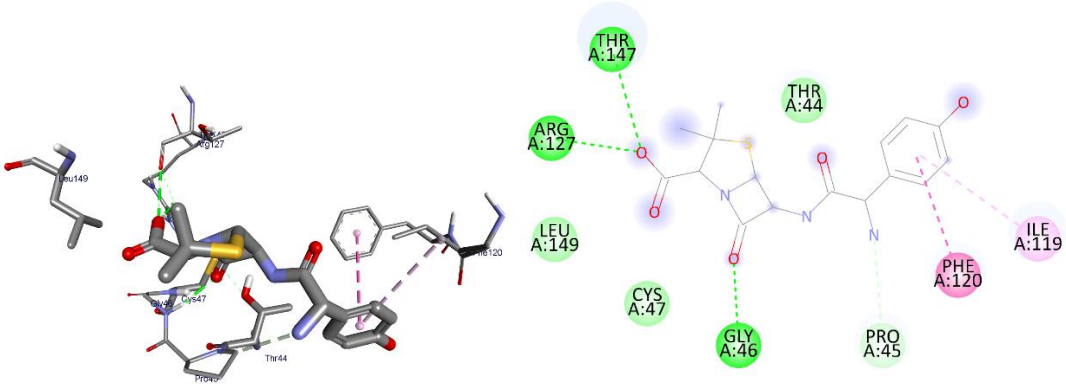

Figure 29: 3D (b) and 2D (a) representations of the binding interactions of amoxicillin against human peroxiredoxin 5 (PDB ID: 1HD2).

4.7 In Silico Prediction of Drug-Likeness, and Pharmacokinetic Prediction Study

Drug-likeness is a prediction that determines whether a specific organic molecule has qualities that indicate it could be an orally active drug (Lipinski, et al. 2001). The isolated compounds' drug-likeness was assessed using "Lipinski's rule of five," which specifies that prospective molecules should have (MW≤500, ilog P≤5, H-bond donors ≤5, and H-bond acceptors ≤10) (Lipinski, et al. 2001) and Veber's parameters (TPSA ≤140 $Å^2$ and rotatable bonds≤10) (Veber, et al. 2002). Compounds **48, 50**, and **51** fulfill Lipinski's rule of five, indicating that they are drug-like and potentially orally active (**Table 18**). Furthermore, all the isolated compounds showed relatively better bioavailability scores of 0.55, indicating drug-like characteristics (Martin 2005). Their HBD values are <3, indicating greater solubility in cellular membranes, and their HBA values range from 1 to 5. The ilog P values for all compounds are less than five, with compounds **50** and **51** having particularly good lipophilic characteristics, indicating a favorable balance between solubility and permeability. The TPSA values of the compounds ranged from 20.23 to 86.99, which is less than 140$Å^2$, indicating that intestinal absorption is good and that the drug does not have passive cellular permeability if the limits are higher than the score (Turner et al. 2004). Using the formula %Abs= 109 -0.345TPSA (Remko 2009), the percentage absorption analysis of the compounds (**Table 18**) revealed that all of the isolated compounds had higher percent absorption than the control. Their molar refractive index values, which range from 34.59 to 123.14, indicate the likelihood that they could be developed to drugs.

Table 18: Calculated parameters of *in silico*bioavailability (drug-likeness) prediction & physicochemical properties of the isolated compounds (**48-51**) and amoxicillin

Compound	MW	NRB	NHBA	NHBD	MR	TPSA	%Abs	iLog P	Log S (ESOL)	Lipinski violations	Synthetic accessibility	Bioavailability score
47	290.35	8	4	0	84.31	48.67	92.21	3.67	-4.44	0	3.27	0.55
48	384.64	4	1	1	123.14	20.23	102.02	4.73	-7.17	1	5.9	0.55
49	124.14	1	2	2	34.59	40.46	95.04	1.31	-1.35	0	1	0.55
50	184.15	2	4	2	41.92	66.76	115.97	1.2	-2.29	0	1.4	0.85
Amoxicillin	365.4	5	6	4	94.56	158.26	54.40	3.17	-0.7	0	6.51	4.17

The ability of molecules to penetrate the outer layer of the skin is described by skin permeability (Kp). The isolated compounds' log Kp values (**Table 19**) were all determined to be within the permissible range of -2.77to -6.71. The SwissADME prediction parameters have shown that the GIA exhibits good oral absorption except for compounds **49**. The results of the BBB permeability test performed on tested compounds (**Table 19**) demonstrated that compounds **49**and **51** lack BBB permeability.

In this study, compound **48** inhibited all cytochrome P_{450}s except for CYP3A4, while the others showed no inhibitory properties except for compounds **49** and **50**, which inhibited CYP2C9 and CYP3A4, respectively (**Table19**). Furthermore, glycoprotein inhibition measurements were used to predict target compound excretion properties. P-gp and cytochrome P_{450} are known to help protect biofilms (gastrointestinal tract or brain) from exogenous substance efflux (biotransformation) to protect tissues (Finch and Pillans 2014). All of the compounds (**48-51**) exhibited no inhibitionof P-gp, so no liver dysfunction effects are expected after administration.

Table 19: Pharmacokinetic (ADME) properties prediction of the isolated compounds (**48-51**)

Compounds	GI abn	BBB per	Pgp sub	CYP1A2 Inhibitor	CYP2C19 Inhibitor	CYP2C9 Inhibitor	CYP2D6 Inhibitor	CYP3A4 Inhibitor	log Kp (cm/s)
48	High	Yes	No	Yes	Yes	Yes	Yes	No	-4.71
49	Low	No	No	No	No	Yes	No	No	-2.77
50	High	Yes	No	No	No	No	No	Yes	-6.71
51	High	No	No	No	No	No	No	No	-6.01
Amoxicillin	Low	No	No	No	No	No	No	No	-9.94

The pharmacokinetics were also evaluated using the boiled egg model, which allowed for the prediction of GI absorption and blood-brain barrier (BBB) penetration with the alignment of lipophilicity (WlogP) and polarity (TPSA) properties. The white region indicated a high likelihood of passive absorption by the gastrointestinal tract, while the yellow region (yolk) indicated a high likelihood of brain penetration. Yolk and white areas did not have to be mutually exclusive. Furthermore, the points were colored blue if it was predicted to be actively effluxed by P-gp (PGP+) and red if it was predicted to be a non-substrate of P-gp (PGP-).

The BOILED-Egg (**Figure 30**) prediction model showed that compound **51** was predicted as passively absorbed but not accessing the brain (in the white) and PGP– (red dot), whereas, compound **48** and **50** was predicted as brain-penetrant (in the yolk) and not subject to active efflux (red dot). Compound **49** was predicted as not absorbed and not brain penetrant (outside the Egg).

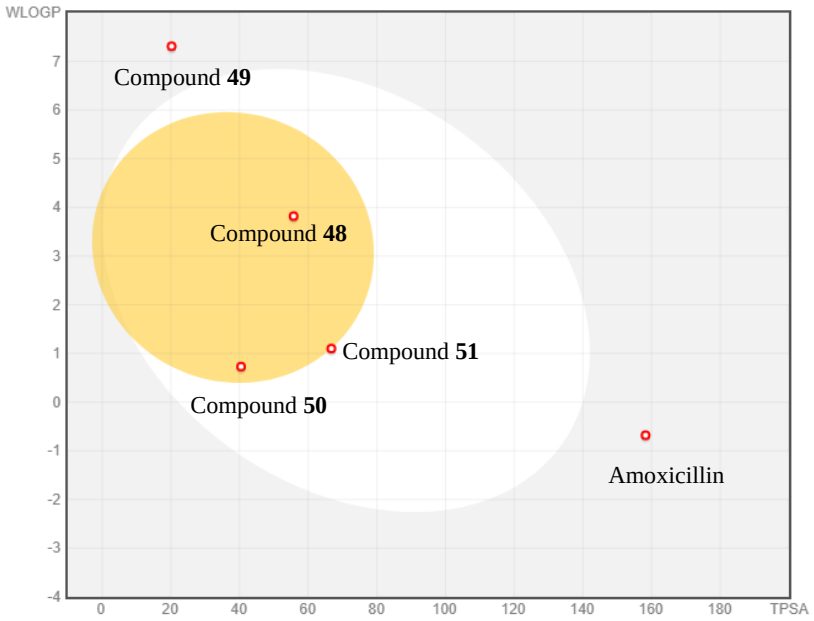

Figure 30: BOILED-Egg model for predicting gastrointestinal absorption and brain access.

All compounds were found to be inactive in all toxicological endpoints except for compounds **48**and **49** that were predicted to be immunotoxin. From the results shown in **Table 20** we can deduce that the compounds can have acceptable profile as a lead for the development of safe and effective drugs in the future. The predicted LD_{50} (mg/kg) for the tested compounds range from 650 to 3800, and their toxicity class as classified by Pro Tox-II ranges from grade 3 to 5.

Table 20: *In silico* pharmacodynamics (toxicity) prediction of compounds (**48-51**) and amoxicillin using Pro Tox-II online servers.

Compounds	Hepatotoxicity	Carcinogenicity	Immunotoxicity	Mutagenicity	Cytotoxicity	LD_{50}(mg/Kg)	Toxicity Class
48	Inactive	Inactive	Active	Inactive	Inactive	3800	5
49	Inactive	Inactive	Active	Inactive	Inactive	890	4
50	Inactive	Inactive	Inactive	Inactive	Inactive	650	3
51	Inactive	Inactive	Inactive	Inactive	Inactive	1800	4
Amoxicillin	Inactive	Active	Inactive	Inactive	Inactive	2991	4

5. CONCLUSION AND RECOMMENDATION

5.1 Conclusion

Natural products represent an important source of new lead compounds in drug discovery research. The present study identified one caffeic acid derivative (**48**), desmosterol (**49**), two phenolic derivatives (**50**, **51**) and two disaccharides (**51**, **52**). All compounds reported herein for the first time from the species. Promising inhibition zone values were observed by chloroform extract against *K. pneumoniae* (13±0.00 mm), *S. typhimurium* (13±1.00 mm), and *S. aureus* (12.33±0.58 mm) compared to gentamycin (15.86±4.67 mm, 28.86±2.34 mm, and 25.43±2.15 mm, respectively). Compound **49**and **51**showed significant activity against *P. aeruginosa* with a mean inhibition zone of 14±1.00 mm and 14±1.73 mm, respectively, compared to gentamycin (25±2.52 mm). Compound **49** also displayed promising inhibition against *S. typhimurium* with a mean inhibition zone value of 15±0.00 mm. The results from DPPH activity demonstrated chloroform and methanol extracts inhibited the DPPH radical by 95.14 % and 72.98 % whereas compound **49** displayed 35.69 % inhibition. The drug-likeness analysis showed that compounds **48, 49,** and **51** satisfy Lipinski's rule of five with zero violations. Compounds **49** and **50** showed binding affinities of -6.3 and -6.7 against *E. coli* DNA gyrase B, respectively, while **49** showed -7.8 kcal/mol against PqsA, compared to amoxicillin (-6.1 kcal/mol and -7.3 Kcal/mol, respectively). The LD_{50} and toxicity class values obtained by *insilico* toxicity profile analysis of the compounds suggested that none of the compounds has hepatotoxicity, mutagenicity, and cytotoxicity. The docking binding affinity and *in vitro* assay results suggest that compound **49**can be considered as potential antibacterial agents against tested organisms. Compounds **48**and **49** can be considered promising free radical scavengers. Therefore, the *in vitro* antibacterial and radical scavenging activity, and the molecular docking analysis suggest the potential use of the extracts of *G. superba* and compounds **48, 49**and **51** as promising antibacterial agents and the extracts as promising free radical scavengers.

5.2 Recommendation

Further biological activity (antifungal, anticancer, and cytotoxicity) on crude extracts as well as isolated compounds are required to validate the traditional use of the plant. Additionally, 2D NMR spectroscopic techniques (HMBC, HSQC, COSY, and NOESY) and MS studies are required to have a better understanding of structural and chemical parameters required to develop related drug lead compounds.

REFERENCES

Abdullahi, R., Abubakar, and Haque Mainul. (2020). "Preparation of Medicinal Plants: Basic Extraction and Fractionation Procedures for Experimental Purposes." *Journal of Pharmacy and BioAllied Science* 1-10.

Abebe, D. (1986). "Traditional medicine in Ethiopia: the attempts being made to promote it for effective and better utilization." *SINET.*

Alams, K., Skaug, N., & Ahmad, I. (2005). An in vitro antimicrobial comparison of miswak extract with commercially available non-alcohol mouthrinses. *International Journal of Dental Hygine, 3*, 18–24.

Amritpal, Singh Saroya. (2011). *Herbalism, Phytochemistry and Ethnopharmacology.* Enfield, New Hampshire: Science Publishers.

Annika, Vinnersten, and Larsson Sonny. (2010). "Colchicine is still a chemical marker for the expanded Colchicaceae." *Biochemical Systematics and Ecology* 38 (6): 1193-1198.

Ayele, Tamrat Tesfaye. (2018). "A Review on Traditionally Used Medicinal Plants/Herbs for Cancer Therapy in Ethiopia: Current Status, Challenge and Future Perspectives." *Organic Chemistry Current Research* 7 (2): 192.

Bargah, & Rohit. (2015). Preliminary test of phytochemical screening of crude ethanolic and aqueous extract of *Moringa pterygosperma* Gaertn. *Journal of Pharmacognosy and Phytochemistry, 4*(1), 7–9.

Belayneh, A,, and NF. Bussa. (2014). "Ethnomedicinal plants used to treat human ailments in the prehistoric place of Harla and Dengego valleys, eastern Ethiopia." *Journal of Ethnobiol Ethnomed* 10 (1): 18.

Bharat, Goel, Reddy Harichander, Cholkar Anjali, Kumar Sanjeev, Kumar Guru Santosh, and K Jain Shreyans. (2022). "Isolation of a new cytotoxic colchinoid from Gloriosa superba roots." *Natural Products Research* 1-6.

Bharathi, P., D. Philomina, and S. Chakkaravarthi. (2006). "Antimitotic Effect of Colchicine from Six Different Species of Gloriosa in Onion Roots (Allium cepa)." *Journal of Medical Science* 6: 420-425.

Bhargav, Bhide,, and Acharya Rabinarayan. (2012). "Langali (Gloriosa superba) Linn. and its therapeutic importance in Ayurveda - A Review. ." *International Journal of Ayurvedic Medicine* 3 (2): 58-67.

Brand-Williams, Cuvelier, W., M. E., and C. Berset. (1995). "Use of a free radical method to evaluate antioxidant activity." *LWT - Food Science and Technology* 28 (1): 25-30.

CLSI. (2018). "CLSI Guideline M02 – Performance Standards for Antimicrobial Disk Susceptibility Tests." 13 ed.

Dar, RA,, M, Shahnawaz, and PH Qazi. (2017). "Natural product medicines: A literature update." *Journal of Phytopharmacology* 6 (6): 349-351.

Dhiman, A., Nanda, A., Ahmad, S., & Narasimhan, B. (2012). In vitro antimicrobial status of methanolic extract of Citrus sinensis Linn. Fruit peel. *Chronicles of Young Scientists., 3*, 204-208.

Edeoga, H.O., D.E. Okwu, and B.O. Mbaebie. (2005). "Phytochemical constituents of some Nigerian medicinal plants." *African Journal of Biotechnology* 4: 685-688.

EUCAST . (2019). "Disk Diffusion Method for Antimicrobial Susceptibility Testing." 7 ed.

Fausto, R., Jessica, G., José, P., Jazmin, M. P., Ajit, K., Gloria, D., et al. (2020). Phytochemical Constituents, Antioxidant, Cytotoxic, and Antimicrobial Activities of the Ethanolic Extract of Mexican Brown Propolis. *Antioxidants, 9*, 70.

Finch, A., and P. Pillans. (2014). "P-glycoprotein and its role in drugdrug interactions." *Australian Prescriber* 37 (4): 137-139.

Gebeyahu, Getaneh, Zemede Asfaw, Abiyu Enyew, and Nagappan Raja. (2014). "Ethnobotonical study of traditional medicinal plants and theri conservation status in mecha werada west gojjam zone of ethiopia." *international journal and pharmaceuticals health care research* 137-154.

GebreEgziabher, TB.,. (1991). "Diversity of Ethiopian Floras. In:." Edited by Hawks JG, Worda M Eagles JM. *Plant Genetic Resource of Ethiopia* (Cambridge: Cambridge University Press) 75-81.

Hafidh, R., Abdulamir, A., Vern, L., Bakar, F., Abas, F., Jahanshiri, F., et al. (2011). Inhibition of growth of highly resistant bacterial and fungal pathogens by a natural product. *The Open Microbiology Journal, 5*, 96–106.

Hassan, AKMS,, and SK. Roy. (2005). "Micropropagation of Gloriosa superba L. through High Frequency Shoot." *Proliferation. Plant Tissue Cult.* 15: 67-74.

Itefa, Degefa, ALEMU, and Muleta, Daba Tolessa. (2016). "Gloriosa, a source of colchicine꞉review article." *International Journal of Biological and Chemical Sciences* 10 (4): 1888-1893.

Jana, S,, and GS. Shekhawat. (2011). "Critical review on medicinally potent plant species: Gloriosa superba." *Fitoterapia* 82: 293-301.

Jayakumar, Fairen Angelin, Simon Samson Eugin, Yan Yi Wei, and Yap Pui Woon. (2018). "Characteristic and Optimized Use of Bioactive Compounds From *Gloriosa superba* and Albizia Amara with Apoptotic Effect on Hepatic and Squamous Skin Carcinoma." *International Journal of Pharmaceutical Sciences and Research* 9 (5): 1769-1778.

John, JC,, J, Fernandes, T, Nandgude, SR, Niphade, A, Salva, and PT. Deshmukh. (2009). "Analgesic and anti-inflammatory activities of the hydroalcoholic extract from Gloriosa superba Linn." *International Journal of Green Chemistry* 3 (3): 215-219.

Jothi, Chimahali, Jebamalar Anjelin, Duraikannu Gajalakshmi, And Thirumal Sivakumar. (2019). "Phytochemical Analysis and Evaluation of Antimicrobial Activity In The Whole Plant Extracts of Gloriosa Superba." *Asian Journal of Pharmacy and Clinical Research* 12 (6): 245-249.

Kamal, T., Muzammil, A., Akintunde, R., Rahma, M., & Omar, M. (2012). Preliminary phytochemical screening test of Garcinia griffithii Plant. *Innova Cienta*, *4*(4l).

Kelbessa, E, S Demissew, Z Woldu, and S Edwards. (2000). "Some threatened Endemic plants of Ethiopia. In The status of some plants in parts of tropical Afric." *East and Central Africa: NAPRECA* 35-55.

K. Gopinath, C. Karthikeyan, A.S. Haja Hameed, K. Arunkumar and A. Arumugam, (2015). "Phytochemical Synthesis and Crystallization of Sucrose from the Extract of *Gloriosa superba"*. *Research Journal of Phytochemistry, 9:* 144-160.

Khan, H,, MA, Khan, T, Mahmood, and MI. Chaudhary. (2008). "Antimicrobial activities of Gloriosa superba Linn (colchicaceae) extract. ." *Journal of Enzyme Inhibition and Medicinal Chemistry* 23 (6): 855-859.

Khan, H.,, M.A. Khan, and I. Hussan. (2007). "Enzyme inhibition activities of the extracts from rhizomes of Gloriosa superba Linn (Colchicaceae). ." *Journal of Enzyme Inhibition and Medicinal Chemistry* 6: 722-725.

Kumar, C. G., Mongolla, P., Pombala, S., Bandi, S., Babu, K. S., & Ramakrishna, K. V. S. (2017). "Biological evaluation of 3-hydroxybenzyl alcohol, an extrolite produced by Aspergillus nidulans strain KZR-132." *Journal of Applied Microbiology*, 122(6), 1518–1528.

Kumarasamy, Y., Maureen, B., Philip, J. C., Marcel, J., Lutfun, N., & Satyajit, D. S. (2007). Screening seeds of some Scottish plants for free radical scavenging activity. *Phytochemical research, 21*, 615-621.

Kumaraswamy, MV,, HV, Kavitha, and S, Satish. (2008). "Antibacterial Evaluation and Phytochemical Analysis of Betula utilis D. Don Against Some Human Pathogenic Bacteria." *Advances in Biological Research* 2 (1-2): 21-25.

Latha, K.P.,, H. Kirana, and H.N. Girish. (2013). "Anti- Implantation Activity of the Hydroalcoholic Tuber Extract of Gloriosa superba Linn in Female Albino Rats." *International Journal of advances in Pahrm. Bio. and Chem* 2 (3): 443-448.

Legrand, S., Nordlander, G., Nordenhem, H., Borg-Karlson, A K., Unelius, C R. (2004). "Hydroxy-Methoxy benzoic methyl esters: Synthesis and antifeedant activity on the pine weevil, Hylobius abietis."*Zeitschrift für Naturforschung. B, A Journal of Chemical Sciences*, 59(7): 829-835

Lipinski, C.A.,, F., Lombardo, B.W. Dominy, and P.J., Feeney. (2001). "Experimental and computational approaches to estimate solubility and permeability in drug discovery and development settings." *Advanced drug delivery reviews* 46 (1-3): 3-26.

Lipinski, CA,. (2016). "Rule of five in 2015 and beyond: Target and ligand structural limitations, ligand chemistry structure and drug discovery project decisions." *Advanced Drug Delivery Reviews* 101: 34–41.

Maroyi, Alfred, and L.J.G. van der Maesen. (2012). "Revision of Gloriosa L. (Colchicaceae)." In *The genus Gloriosa (Colchicaceae) – ethnobotany, phylogeny and taxonomy*, 77-148.

Maroyi, Alfred. (2012). *The genus Gloriosa (Colchicaceae) – ethnobotany, phylogeny and taxonomy*. Wageningen, NL: Wageningen University, .

Martin, Y. C. (2005). "A bioavailability score." *Journal of Medicinal Chemistry* 48 (9): 3164–3170.

Michael, A. Arnold. (2011). *Landscape Plants For Texas And Environs,*. 4.

Mir, M. A., Parihar, K., Tabasum, U., & Kumari, E. (2016). Estimation of alkaloid , saponin and flavonoid , content in various extracts of *Crocus sativa*. *Journal of Medicinal Plant Studies*, *4*(5), 171–174.

Narramore S, Stevenson CEM, Maxwell A, Lawson DM, and Fishwick CWG. (2019). "New insights into the binding mode of pyridine-3-carboxamide inhibitors of *E. coli* DNA gyrase." *Bioorganic and Medicinal Chemistry* 27: 3546–3550.

Nikhila, GS,, G, Sangeetha, TS Preetha, and TS Swapna. (2016). "GC-MS analysis of phytochemical compounds present in the rhizome of *Gloriosa superba* L." *Journal of Pharmacognosy and Phytochemistry* 5 (5): 17-20.

Nwankwo, I., Onwuakor, C., & Aninweze, O. (2014). Antibacterial activity of Ethanolic extracts of *Citrus sinensis* peels on *Staphylococcus aureus Pseudomonas aeruginosa* isolated from wound infections. *International Journal of Advances in Pharmacy, Biology and Chemistry, 3(4)*, 941–947.

Nwodo, O., & Nkwocha, P. (2015). Qualitative and Quantitative Phytochemical Screening of the Aqueous Leaf Extract of *Senna mimosoides* : Its Effect in in vivo Leukocyte mobilization induced by inflammatory stimulus. *International Journal of Current Microbiology and Appliied Science*, *4*(5), 1176–1188.

Patil, P.B., and R.T. Gavade. (2012). "*Gloriosa superba* Linn – A medicinally important plant." *Annals of Pharmacy and Pharmaceutical Science* 3 (2): 72-74.

Pawar, B.M., Vishal Wavhal, N.D. Pawar, M.R. Agarwal, P.B. Shinde, and H.V.. Kamble. 2010. "Anthelmintic activity of *Gloriosa superba* Linn (Liliaceae)." *International Journal of PharmTech Research* 1483-1487.

Praiwala, B., Priyanka, S., Raghu, N., Gopenath, N., Gnanasekaran, A., Karthikeyan, M., Indumathi, R., Ebrahim, N. K., Pugazhandhi, B., Pradeep, P., Ranjith, M. S., Balasubramanian, S., & Basalingappa, K. M. (2019). In vitro anti-bacterial activity of Tinospora cordifolia leaf extract and its phytochemical screening. *Journal of Biomedical Sciences*, *5*(2), 10–17

Pulliah, T.,. (2002). *Medicinal plants in India.* Vol. 1. New Delhi: Regency Publications.

Rahman, S., Parvez, A. K., Islam, R., & Khan, M. H. (2011). Antibacterial activity of natural spiceson multiple drug resistant *Escherichia coli* isolated from drinking water. *Bangladesh Annals of Clinical Microbiology and Antimicrobials, 10*, 10.

Rani, VU, M, Sudhakar, A, Ramesh, BVS, Lakshmi, and Y. Srinivas. (2016). "Protective effect of hydroalcoholic extract of *Gloriosa superba* Linn in lead induced neurotoxicity in rats." *International Journal of Pharmacy* 6 (2): 257-266.

Rehana banu, H., and N Nagarajan. (2012). "Phytochemical screening for active compounds in Gloriosa superba leaves and tubers." *International Journal of Pharmacognosy and Phytochemical Research* 4 (1): 17-20.

Remko, M. (2009). "Theoretical study of molecular structure, pKa, lipophilicity, solubility, absorption, and polar surface area of some hypoglycemic agents." *Journal of Molecular Structure* 897 (1-3): 73-82.

Sachin, Chaudhary, El-Shorbagi Abdel-Nasser, Shridhar Bhawna, Kumar Gupta Mandeep, and Chandra Verma Harish. (2019). "A Review on Phytochemical And Pharmacological Profile of *Gloriosa superba* Linn." *International Research Journal of Pharmacy* 10 (4).

Salim, A. A., M.J. Garson, and D.J. Craik. (2004). "New Alkaloids from Pandanus amaryllifolius." *J. Nat. Prod* 67: 54-57.

Sanjay, Jagtap, and Satpute Rajendra. (2014). "Phytochemical Screening, Antioxidant, Antimicrobial and Flavonoid Analysis of *Gloriosa superba* Linn. Rhizome Extracts." *Journal of Academia and Industrial Research (JAIR)* 3 (6): 247-254.

Saraswathi, Umavathi,, Gopinath Kasi, M.S. Manjula, Balalakshmi Chinnasamy, and Arumugam Ayyakannu. 2020. "*Gloriosa superba* L: A critical Review of Recent Advances." *Abasyn Journal of Life Sciences* 3 (2): 48-65.

Sebsebe, Demissew, and Nordal Inger. (2010). *Aloes and Lilies of Ethiopia and Eritrea.*

Seeliger, D,, and BL de Groot. (2010). "Ligand docking and binding site analysis with PyMOL and Autodock/Vina." *Journal of Computer-Aided Molecular Design* 24: 417–422.

Senthilkumar, M. (2013). "Phytochemical Screening and Antibacterial Activity of *Gloriosa superba* Linn." *International Journal of Pharmacognosy and Phytochemical Research* 5 (1): 31-36.

Shalaka, S. Rokade, A. Joshi, Komal, Mahajan Ketakee, Patil Saniya, Geetanjali. Tomar, S. Dubal Dnyanesh, Singh Parihar, Vijay, Kitture, Rohini, R. Bellare, Jayesh, and Ghosh Sougata. (2018). "*Gloriosa superba* Mediated Synthesis of Platinum and Palladium Nanoparticles for Induction of Apoptosis in Breast Cancer." *Bioinorganic Chemistry and Applications.*

Shanmugam, H., R. Rathinam, A. Chinnathambi, and T. Venkatesan. (2009). "Antimicrobial and mutagenic properties of the root tubers of *Gloriosa superba* linn (Kalihari), Pak. J. Bot., 41(1), 2009, 293-299.(Kalihari),." *Pak. J. Bot.* 41 (1): 293-299.

Simon, SE, and FA Jayakumar. (2016). "Antioxidant Activity and Anticancer Study on Phytochemicals Extract from Tubers of *Gloriosa superba* against Human Cancer Cell (Hep-G2)." *Journal of Pharmacognosy and Phytochemistry* 4 (4): 7-12.

Solomon, Tesfaye, Asres Kaleab, Lulekal Ermias, Alebachew Yonatan, Tewelde Eyael, Kumarihamy Mallika, and Muhammad Ilias. (2020). "Ethiopian Medicinal Plants Traditionally Used for the Treatment of Cancer, Part 2: A Review on Cytotoxic, Antiproliferative, and Antitumor Phytochemicals, and Future Perspective." *Molecules* 25: 4032.

Svatava, Dvoráčkováa,, Sedmerab, Petr, Potěšilováa, Helena, Šantavýa František, and Šimáneka Vilím. (1984). "Alkaloids of Gloriosa superba L." *Collection of Czech. Chemical Community* 49 (6): 1536-1542.

Tadeg H, M. E.-M. (2005). "Antimicrobial activities of some selected traditional Ethiopian medicinal plants used in the treatment of skin disorders. ." *International Journal of Ethnopharmacology* 68-75.

Takenaka, M., Yan, X., Ono, H., Yoshida, M., Nagata, T., & Nakanishi, T. (2003). “Caffeic Acid Derivatives in the Roots of Yacon (*Smallanthus sonchifolius*).” *Journal of Agricultural and Food Chemistry, 51(3), 793–796.*

Thi, P. A. Nguyen, Kim Jung Sung, and Kim Joo-Hwan. (2013). "Molecular phylogenetic relationships and implications for the circumscription of Colchicaceae (Liliales)." *Botanical Journal of the Linnean Society* 172: v.

Trott, O,, and AJ Olson. (2010). "AutoDock Vina: improving the speed and accuracy of docking with a new scoring function, efficient optimization, and multithreading." *Journal of Computational Chemistry* 31: 455–461.

Tulika, Mishra, and Sharma Pallavi. (2020). "A Critical Review of Glory Lily: A Rare Medicinal Plant." *World Journal of Pharmacy and Pharmaceutical Sciences* 9 (10): 1123-1133.

Turner, J.V., D.J. Maddalena, and S. Agatonovic-Kustrin. 2004. "Bioavailability prediction based on molecular structure for a diverse series of drugs." *Pharmaceutical Research* 21 (1): 68-82.

Veber, D. F., S. R. Johnson, H.-Y. Cheng, B. R. Smith, K. W. Ward, and K. D. Kopple. (2002). "Molecular properties that inDuence the oral bioavailability of drug candidates." *Journal of Medicinal Chemistry* 45 (12): 2615–2623.

Warrier, PK, VPK Nambiar, and C. Ramankutty. (1995). *Indian Medicinal Plants.* Edited by Kottakkal Arya Vaidua Sala. Vol. 3. Orient Longman.

Wilson, William K., Rhea M. Sumpter, Joshua J. Warren, Peter S. Rogers, Benfang Ruan, and Jr George J. Schroepfer. (1996). "Analysis of unsaturated c27 sterols by nuclear magnetic resonance spectroscopy." *Journal of Lipid Research* 37: 1529-1555.

World Checklist of Selected Plant Families. n.d. *Kew Science Royal Botanical Garden.* Accessed December 2021. http://wcsp.science.kew.org/qsearch.do.

World Health Organization||WHO Expert Committee on Specifications for Pharmaceutical Preparations. 2018. *Fifty-second report of the WHO Expert Committee on Specifications for Pharmaceutical Preparations.* Publications, Geneva: World Health Organization.

Yancho, Zarev,, Foubert, Kenn, Ionkova, Iliana, Apers, Sandra, and Pieters Luc. (2017). "Isolation and structure elucidation of glucosylated colchicinoids from the seeds of Gloriosa superba by LC-DAD-SPE-NMR." *Journal of Natural Products,* 80 (4): 1187–1191.

APPENDICES

Appendix 1: ^{1}H NMR spectrum of compound **48**

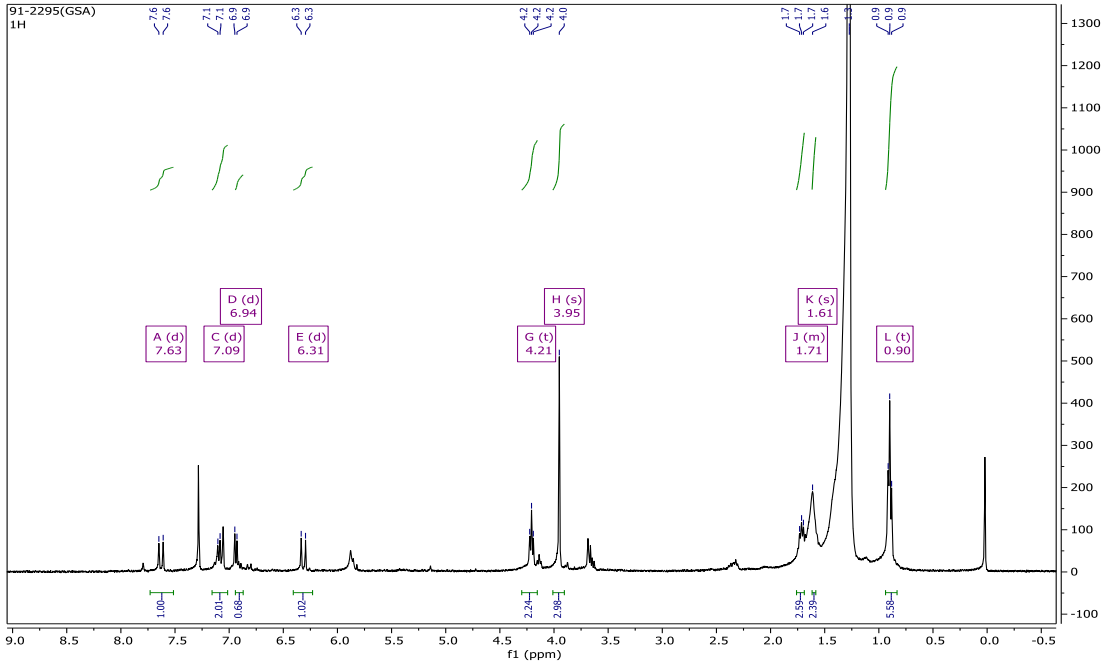

Appendix 2: ^{13}C NMR spectrum of compound **48**

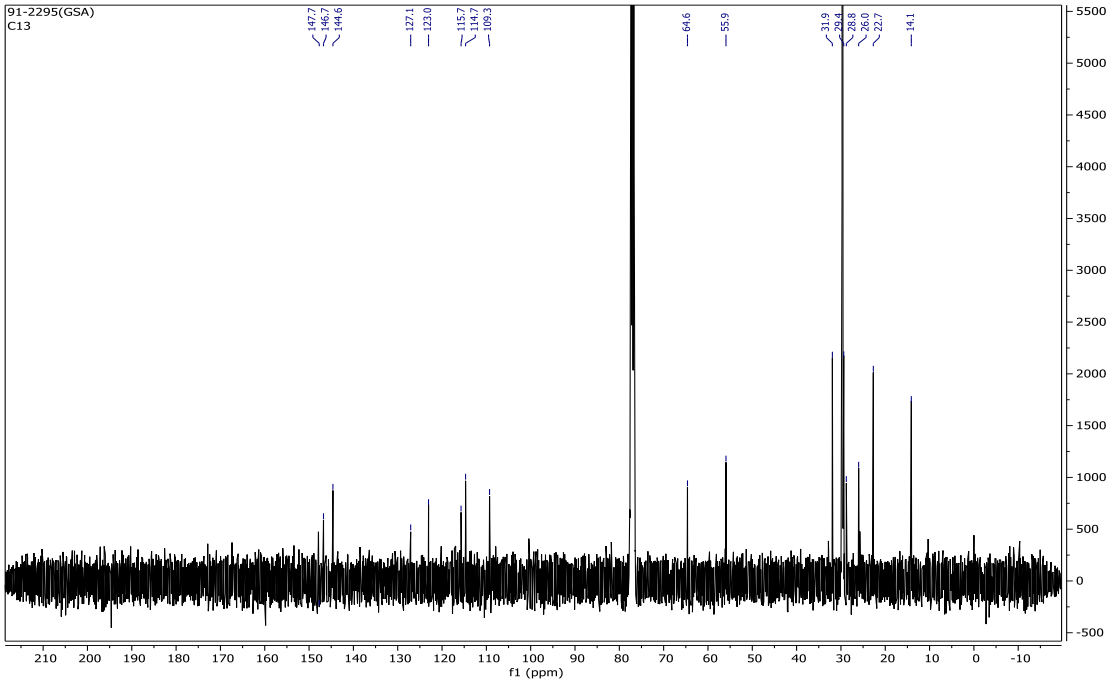

Appendix 3:DEPT-135 spectrum of compound **48.**

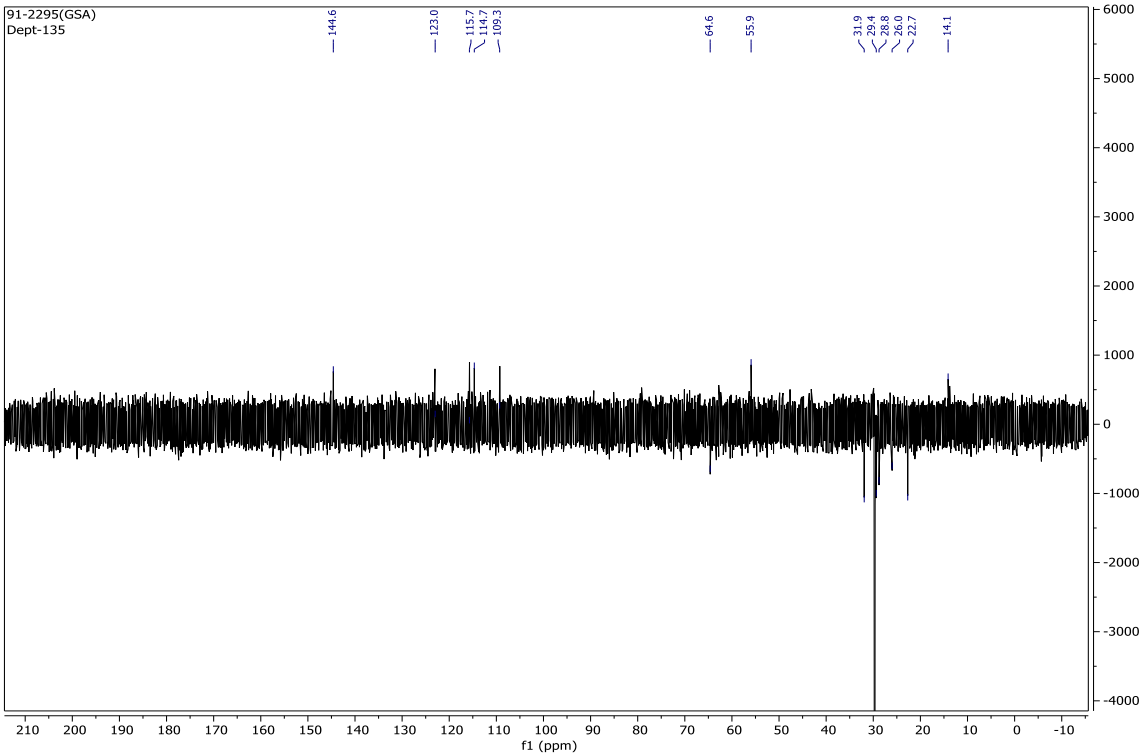

Appendix 4:^{1}H NMR spectrum of compound **49.**

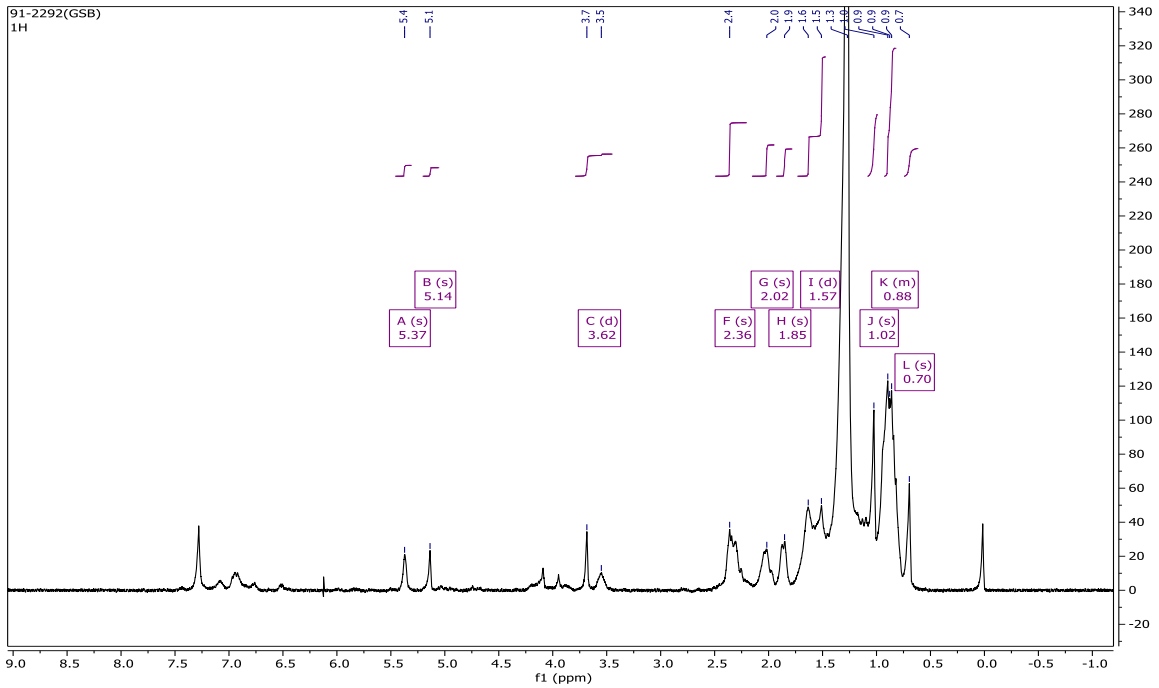

Appendix 5: ^{13}C NMR spectrum of compound **49.**

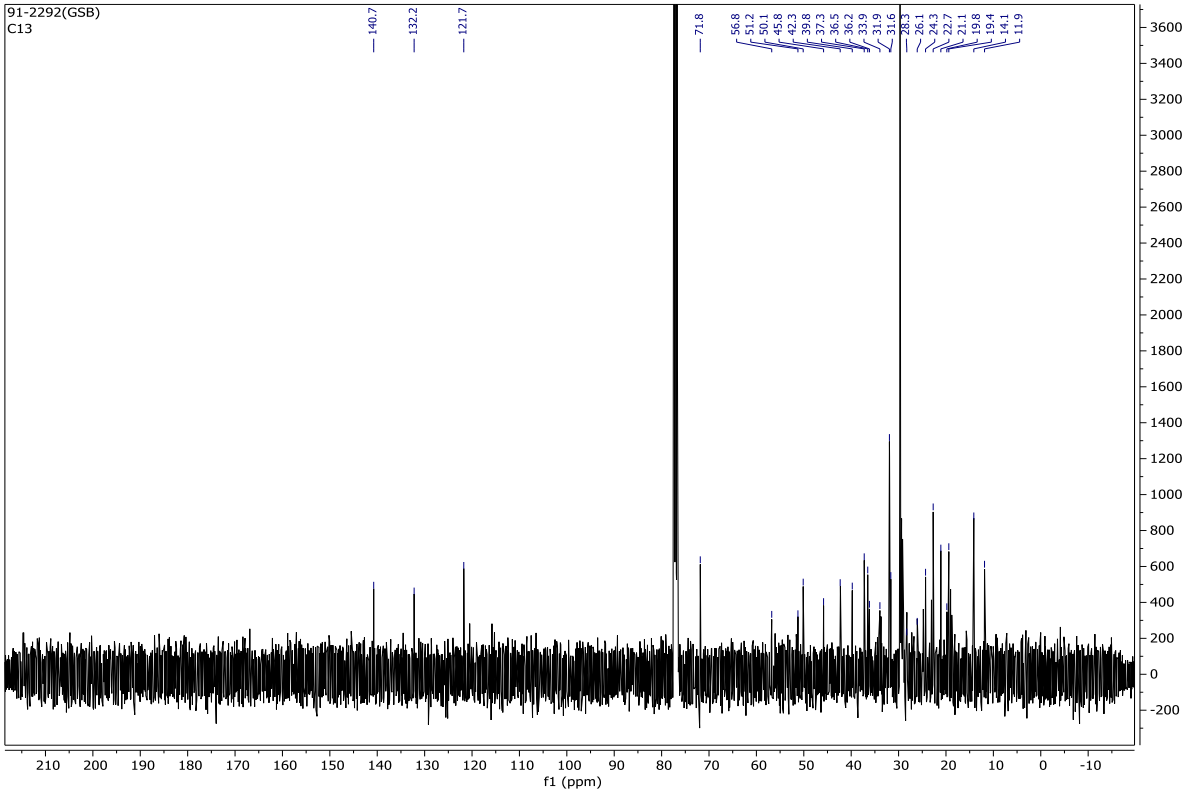

Appendix 6: ^{1}H NMR spectrum of compound **50.**

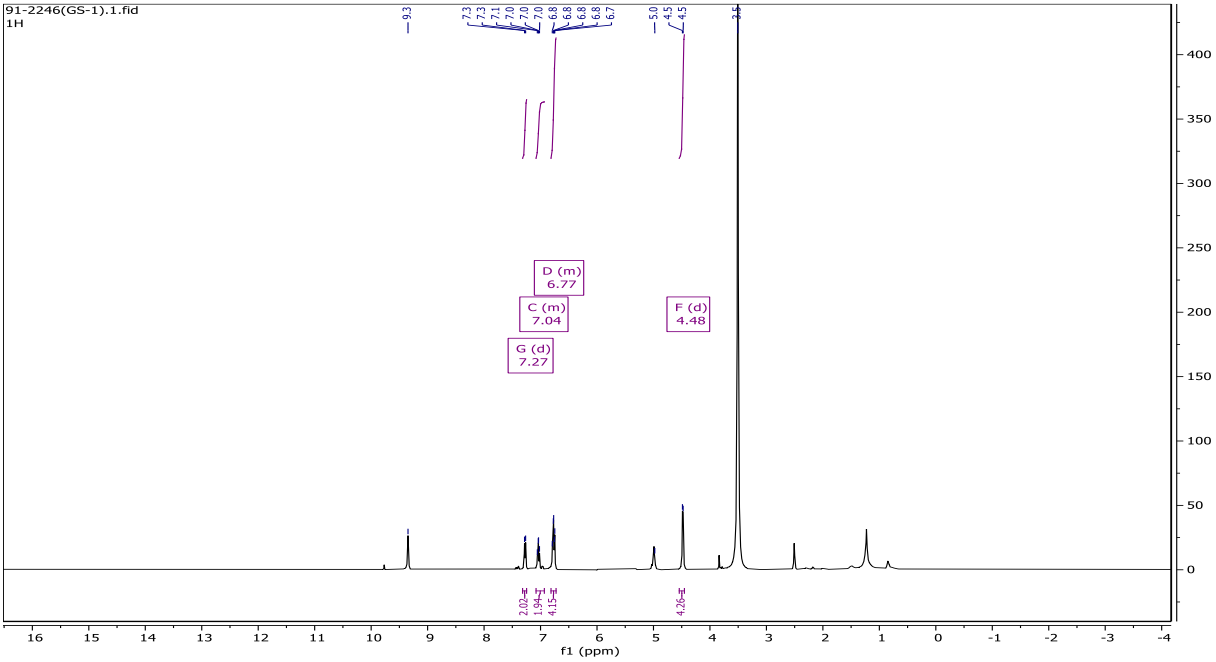

Appendix 7: ^{13}C NMR spectrum of compound **50.**

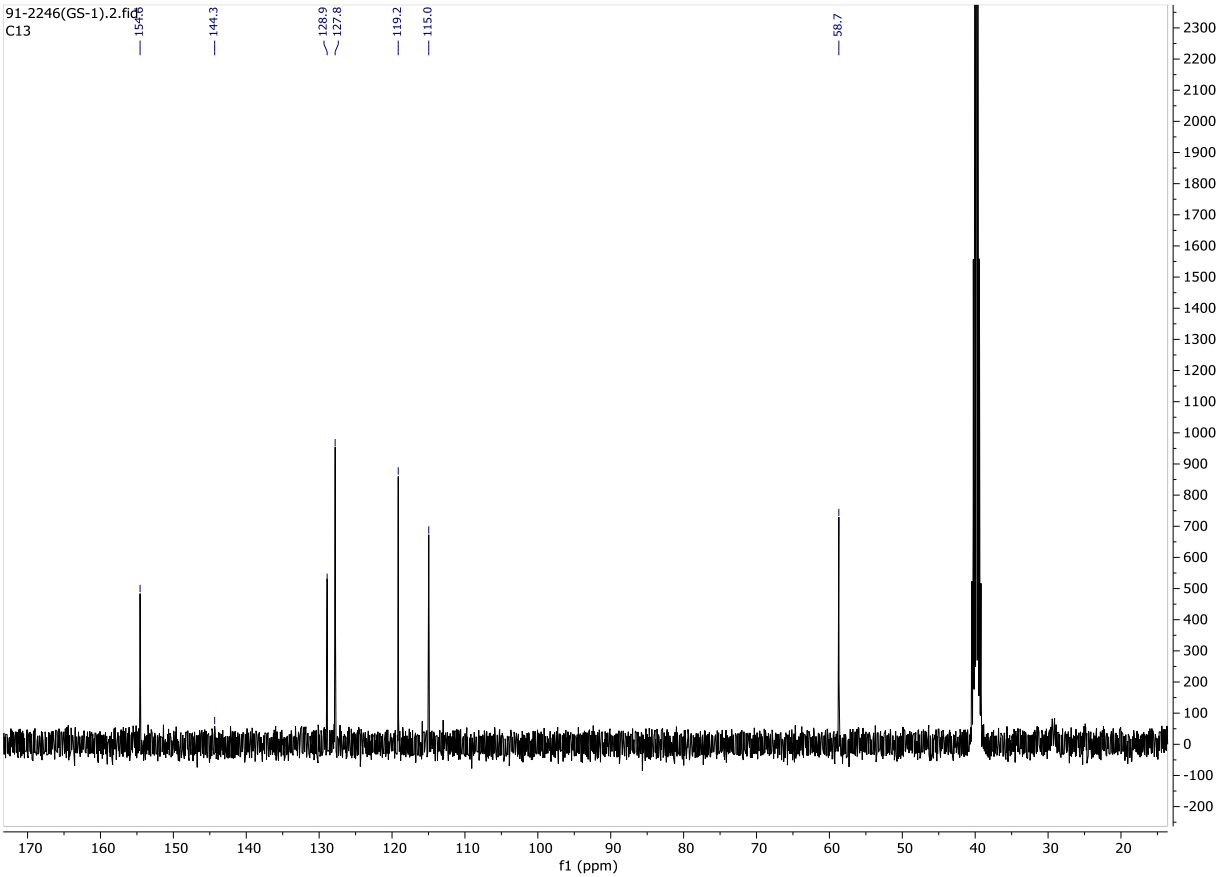

Appendix 8: DEPT-135 spectrum of compound **50.**

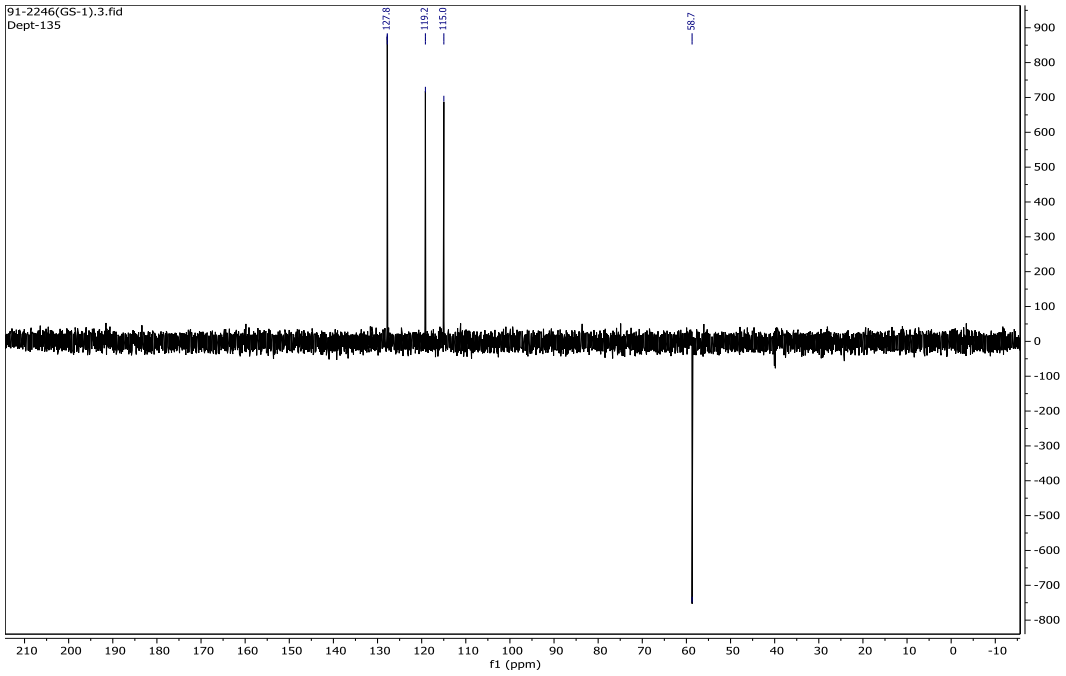

Appendix 9: ^{1}H NMR spectrum of compound **51.**

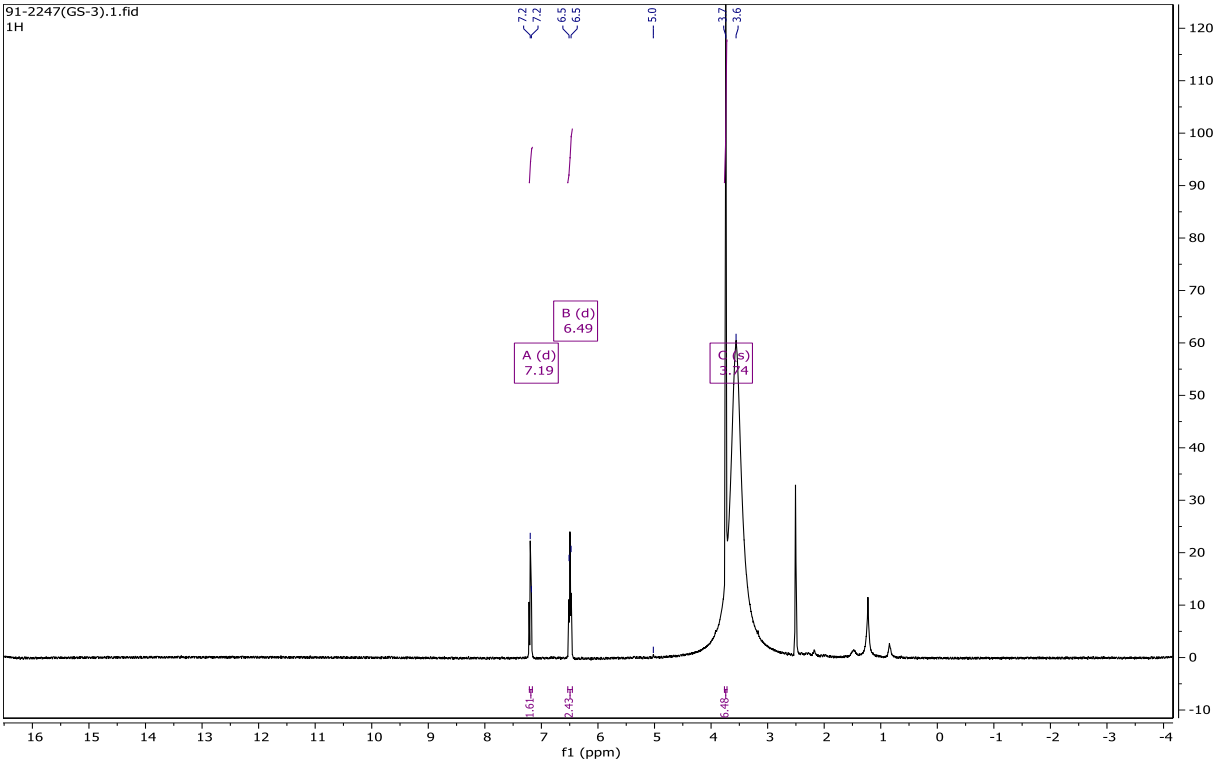

Appendix 10: ^{13}C NMR spectrum of compound **51.**

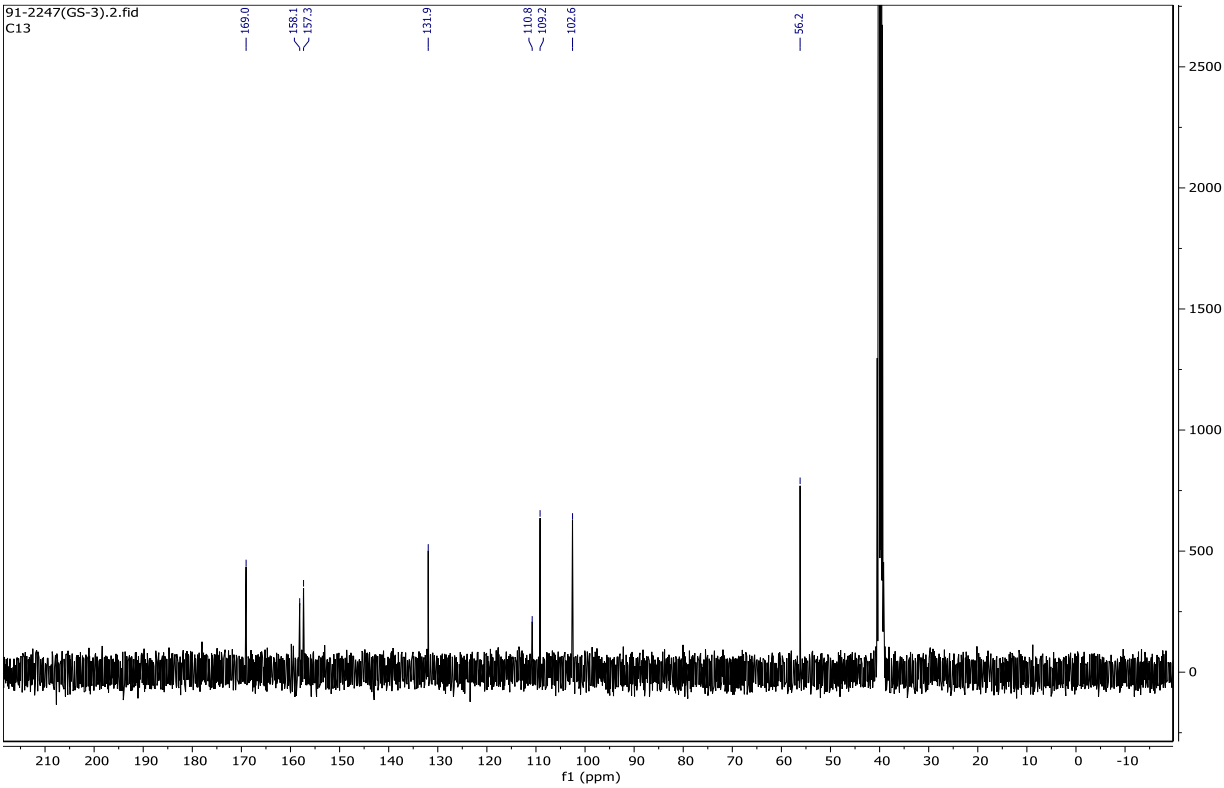

Appendix 11:DEPT-135 spectrum of compound **51.**

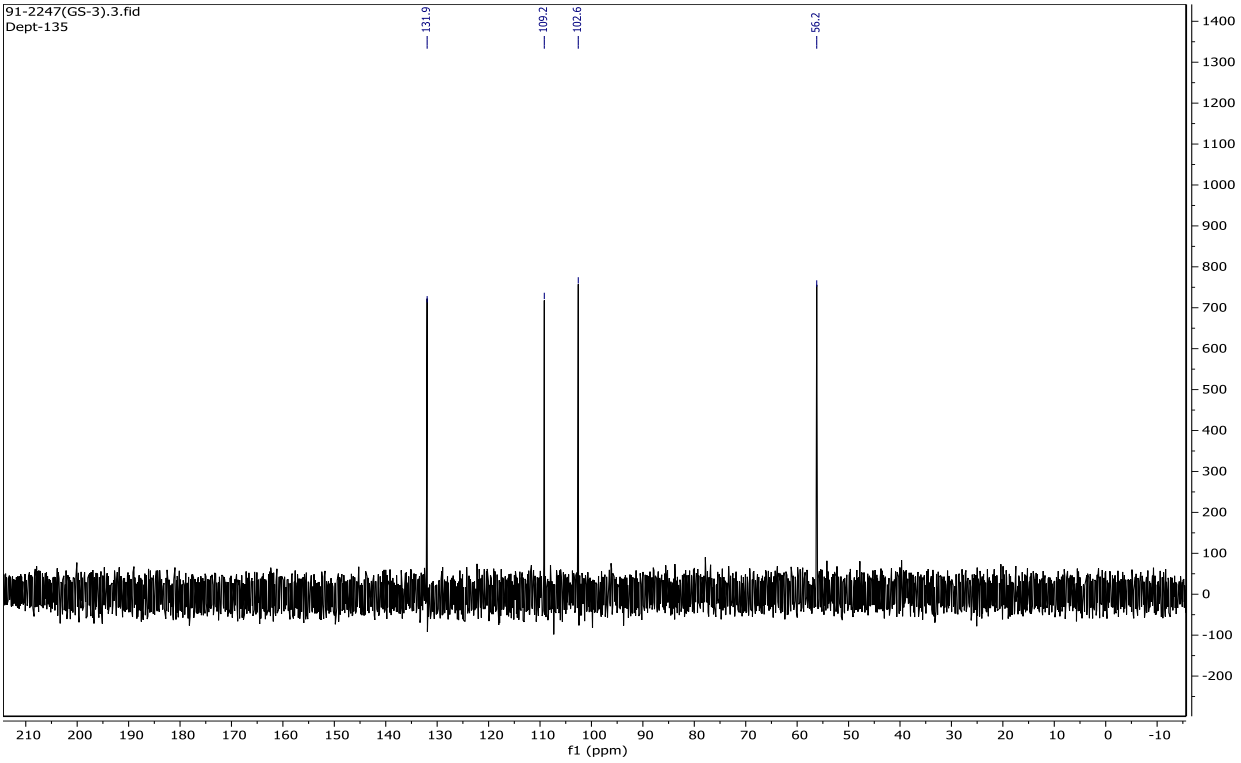

Appendix 12:^{1}H NMR spectrum of compound **52.**

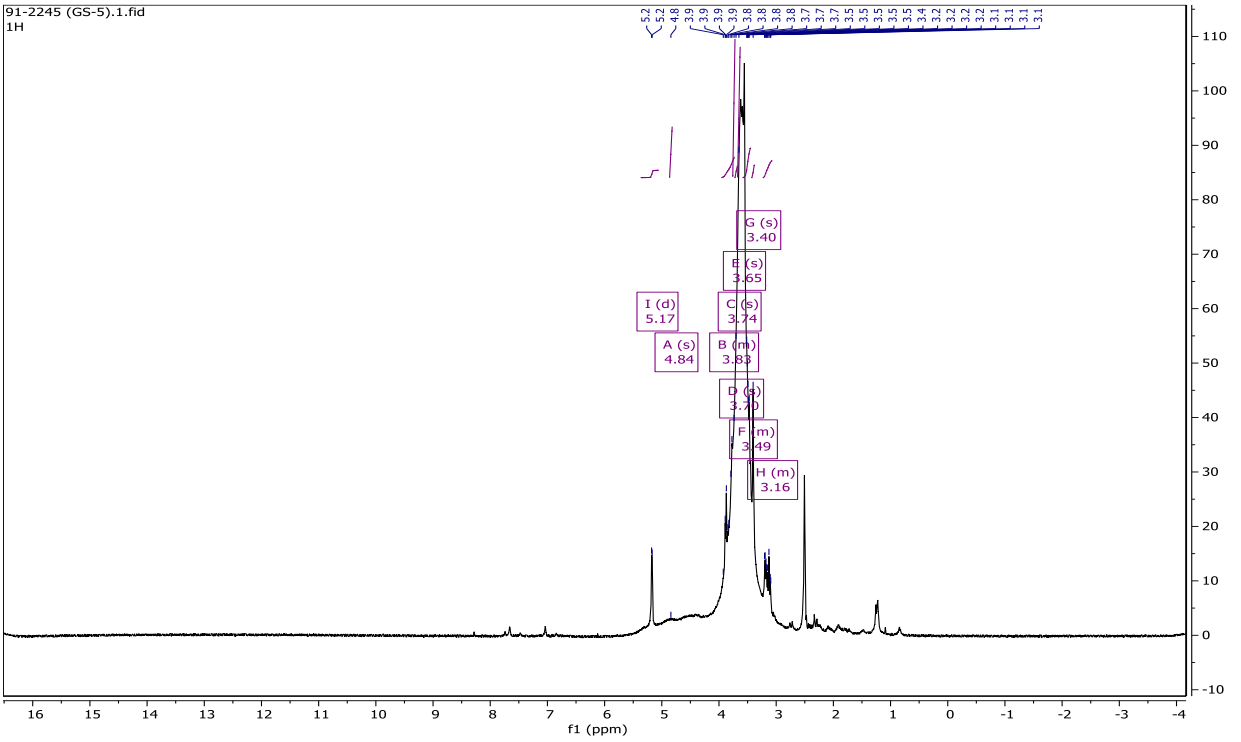

Appendix 13: ^{13}C NMR spectrum of compound **52.**

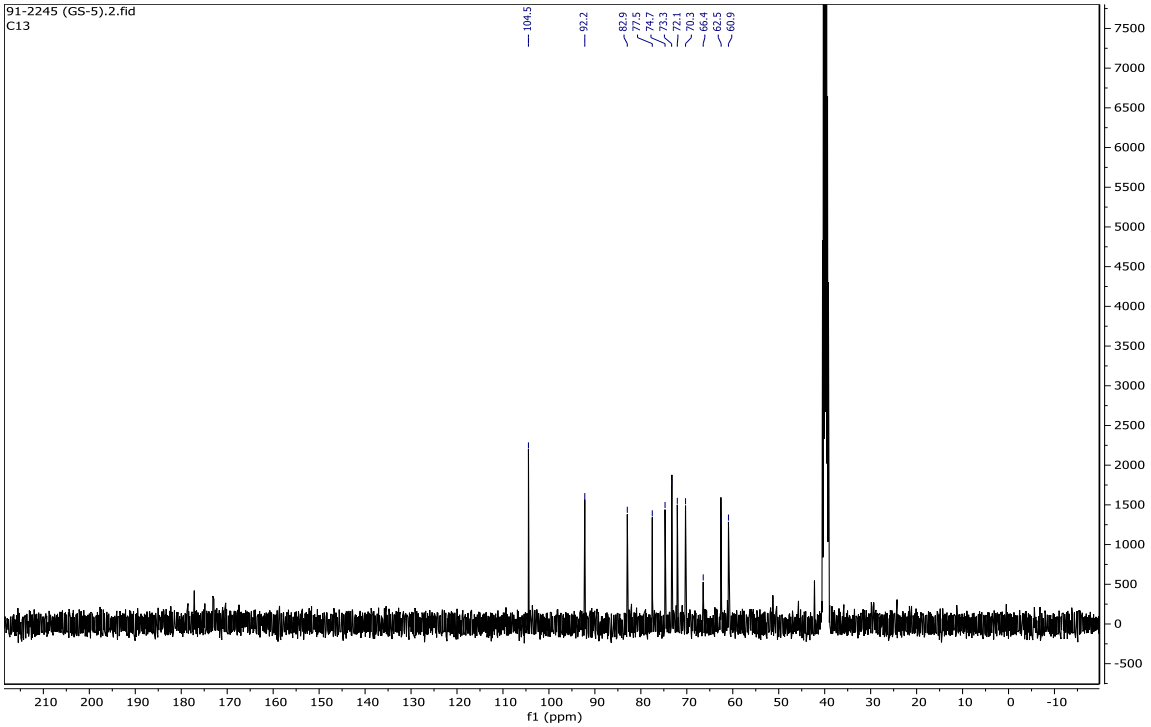

Appendix 14:DEPT-135 spectrum of compound **52.**

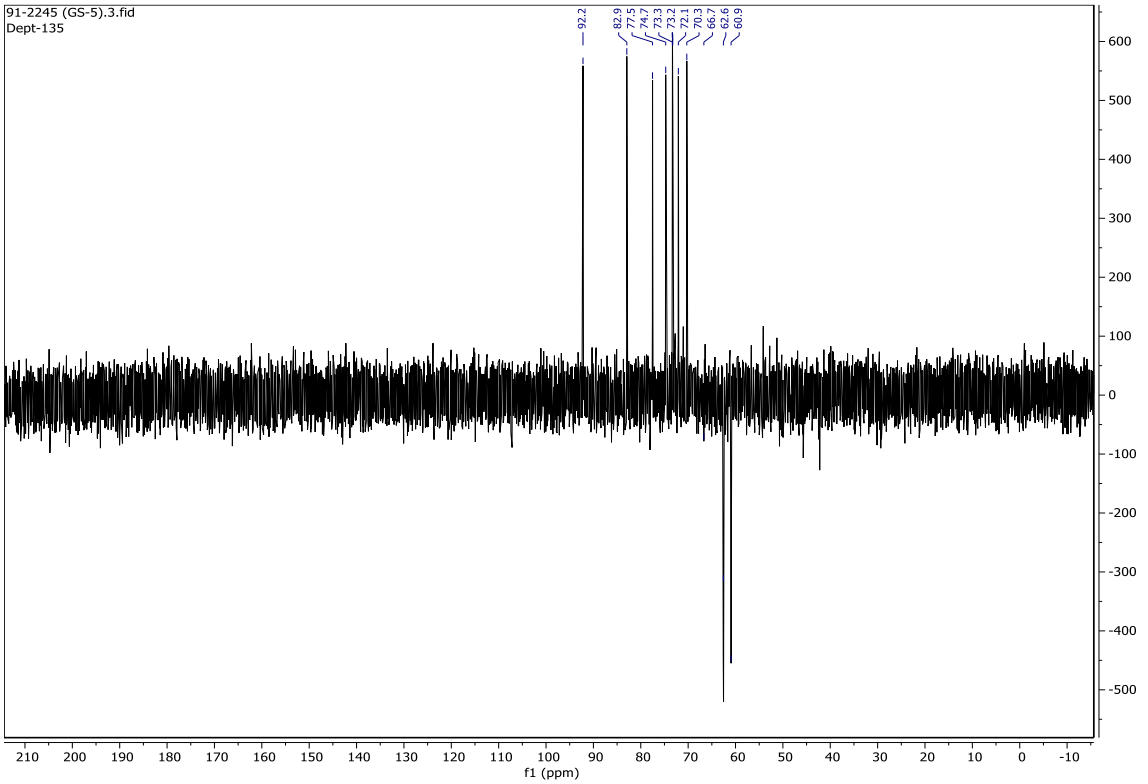

Appendix 15: ^{1}H NMR spectrum of compound **53.**

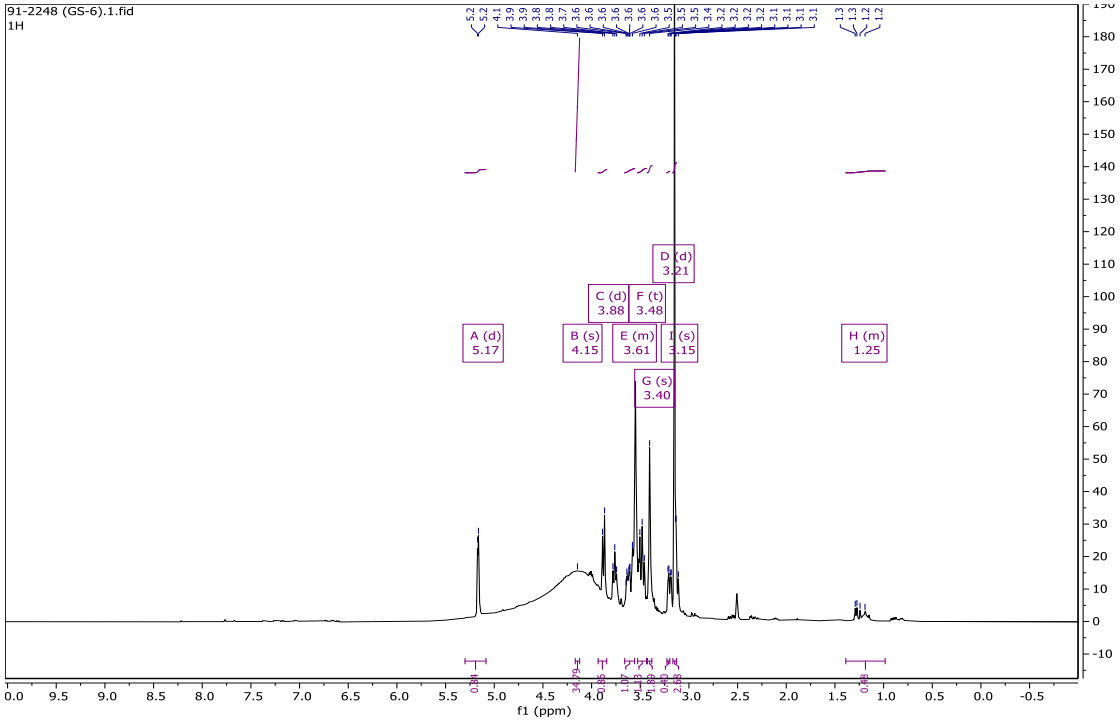

Appendix 16: ^{13}C NMR spectrum of compound **53.**

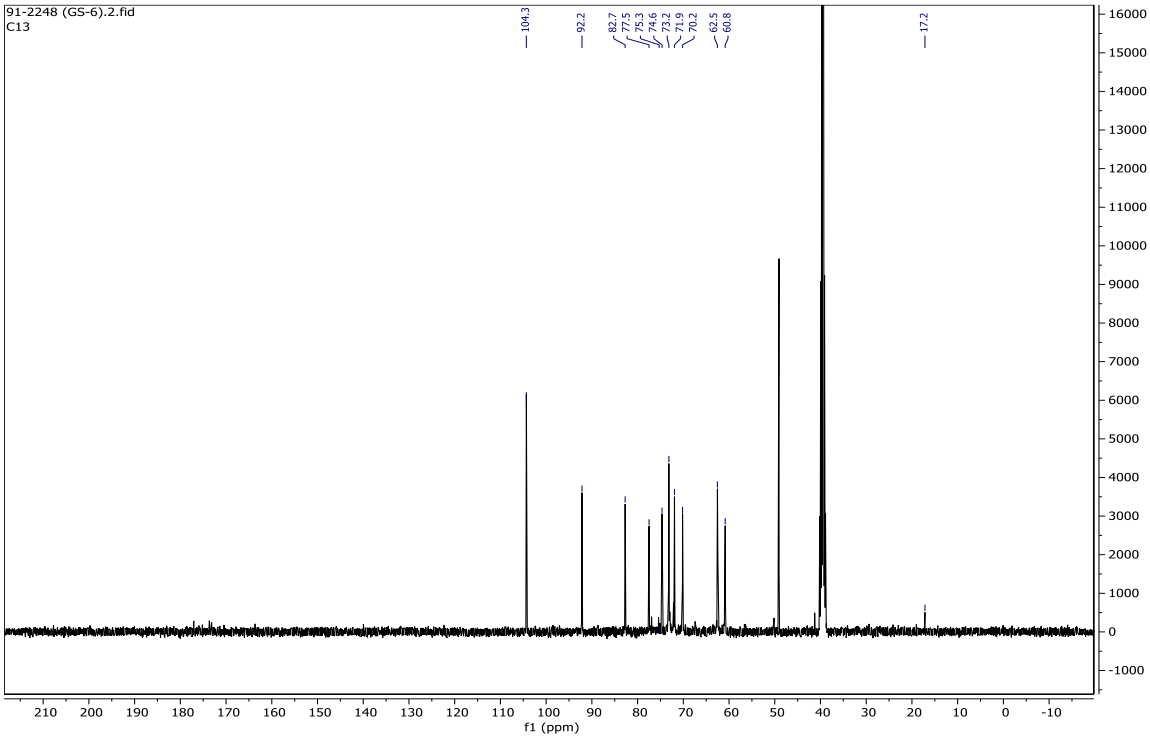

Appendix 17: DEPT-135 spectrum of compound **53.**